Studies on *c*-type cytochromes exhibiting "large g_{max}" / HALS EPR behaviour

Thesis submitted for the degree of *Philosophiae Doctor*

By

Espen Harbitz

Department of Molecular Biosciences
Faculty of Mathematics and Natural Sciences
University of Oslo, MMXI

Series of dissertations submitted to the
Faculty of Mathematics and Natural Sciences, University of Oslo
No. 1106

ISSN 1501-7710

Cover: Inger Sandved Anfinsen.
Printed in Norway: AIT Oslo AS.

Produced in co-operation with Unipub.
The thesis is produced by Unipub merely in connection with the
thesis defence. Kindly direct all inquiries regarding the thesis to the copyright
holder or the unit which grants the doctorate.

“Science is wonderfully equipped to answer the question "How?" but it gets terribly confused when you ask the question "Why?"”

Erwin Chargaff, discoverer of the 1:1 ratio between pyrimidine and purine bases in DNA.

Acknowledgments

The work presented in this PhD thesis has been carried out at the Department of molecular biosciences at the University of Oslo. Financial support for these studies has been provided by the Norwegian Research Council.

I would like to express my gratitude and thanks to my doctoral advisors professor K. Kristoffer Andersson for all his support during the course of my doctoral work, his enthusiasm, care, and all the opportunities he has provided. The opportunities of international collaborations, visiting other laboratories and going to international conferences have been very inspiring. I would also like to thank my co-supervisor Dr rer. nat. Giorgio Zoppellaro for all our fruitful discussions and encouragement.

I would also like to thank my other co-authors; - Kara L. Bren, Thomas Teschner, Volker Schünemann, Solveig Karlsen, David M. Arciero, Stefano Ciurli, Alfred X. Trautwein, Alan B. Hooper, Amy A. Ensign, Ravinder Kaur, Hans-Petter Hersleth, Ulf Ryde and Lars Hederstedt.

My gratitude goes to the chemistry society Proton, for keeping me at the department of chemistry long enough that I got stuck, and to my mother who showed me the wonders of biochemistry by telling inspiring anecdotes when I took my introductory biochemistry courses. This was crucial in my choice of field of study.

I would specially like to thank all my friends and colleagues at the department through all these years. Especially I would like to thank all present and former members of the metalloproteins group for making a top working environment, and our neighbours, the "bacteriocin group".

Finally, I am grateful to my family and friends for constantly believing in me and supporting me throughout these years.

Oslo, June 2011

Espen Harbitz

Contents

Summary

Small soluble *c*-type cytochromes are found in electron transport chains in all domains of life, and have key roles in metabolism. They contain iron atoms bound in the planar haem cofactor. These iron atoms are axially coordinated by one or two amino acid ligands from the protein backbone. There are several amino acids that can serve as axial ligands to the haem iron. Electron paramagnetic resonance (EPR) has been an important tool in determining the amino acid ligation, and has been important for the study of many proteins in the absence of structural information.

The observation that bis-histidine and histidine-methionine ligated haems could exhibit more EPR spectral types complicated the assignment of the axial ligands, and complimentary methods (near infrared magnetic circular dichroism (NIR-MCD)) must be used. In bis-histidine ligated haems, the structural factors governing the EPR spectral types has been elucidated, and the ligands relative orientation is determining of the EPR behaviour. A similar relationship has not been found for histidine-methionine ligated haems.

In this thesis, different aspects of the histidine-methionine ligation have been investigated. The characterisation of *c*-type cytochrome from the methylotroph *Methylosinus trichosporium* OB3b, which shows a typical "large g_{max}" / HALS (Highly Anisotropic or Highly Axial Low Spin) EPR behaviour, is presented. Furthermore, mutational and spectroscopic studies of *c*-type cytochromes from several different bacteria indicate that subtle changes can trigger a change in the EPR spectral type.

At present, it seems evident that the conformation of the axial ligands is not a dominant factor in determining the ligand field around the haem iron in histidine-methionine ligated haems.

Sammendrag

Små vannløselige *c* cytokrommer finnes i elektrontransportkjeder i alle livets domener, og har essensielle roller i metabolismen. De inneholder jernatomer bundet i den plane kofaktoren hem. Disse jernatomene er koordinert av én eller to aksielle aminosyreligander fra proteinkjeden. Det finnes flere aminosyrer med mulighet for å koordinere til hemjernet. Elektron paramagnetisk resonans (EPR) har vært et viktig verktøy for bestemmelse av aminosyreligeringen av jernet, og har vært viktig i studiene av mange proteiner når strukturinformasjon ikke har vært tilgjengelig.

Observasjonen av at histidin-histidin og histidin-metionin ligerte hemgrupper kunne utvise flere typer EPR spektre vanskeliggjorde bestemmelsen av aksielle ligander, og komplementære metoder (som nærinfrarød magnetisk sirkulærdikroisme (NIR-MCD) spektroskopi)) må benyttes. I histidin-histidin ligerte hemgrupper, er de strukturelle faktorene som bestemmer type EPR spekter kjent, og det er histidinenes relative orientering som bestemmer EPR oppførselen. En tilsvarende sammenheng har ikke blitt observert for histidin-metionin ligerte hemgrupper

I denne avhandlingen har forskjellige aspekter ved histidin-metionin ligeringen blitt studert. Karakteriseringen av et *c* cytokrom fra den metanspisende bakterien *Methylosinus trichosporium* OB3b, som har typisk "stor g_{maks}" / HALS (Høyanisotropisk eller Høyaksielt Lav Spinn) EPR oppførsel er presentert. Videre viser mutasjons og spektroskopiske studier av *c* cytokrommer fra flere forskjellige bakterier at selv små forandringer er nok til å endre type EPR oppførsel.

Det virker nå klart at konformasjonen til de aksielle ligandene ikke er en avgjørende faktor for ligandfeltet rundt hemjernet i histidin-metionin ligerte hemgrupper

List of papers

Paper I

Cytochrome c-554 from *Methylosinus trichosporium* OB3b; a protein that belongs to the cytochrome c2 family and exhibit a HALS-type EPR signal
Espen Harbitz, K. Kristoffer Andersson
PLoS One, **2011**, Vol. 6 (7), Article Number: e22014

Paper II

Low-Temperature EPR and Mössbauer Spectroscopy of Two Cytochromes with His-Met Axial Coordination Exhibiting HALS Signals
Giorgio Zoppellaro, Thomas Teschner, Espen Harbitz, Volker Schünemann, Solveig Karlsen, David M. Arciero, Stefano Ciurli, Alfred X. Trautwein, Alan B. Hooper, K. Kristoffer Andersson
CHEMPHYSCHEM, **2006**, Vol. 7 (6), 1258-1267

Paper III

Modulation of the Ligand-Field Anisotropy in a Series of Ferric Low-Spin Cytochrome c Mutants derived from *Pseudomonas aeruginosa* Cytochrome c-551 and *Nitrosomonas europaea* Cytochrome c-552: A Nuclear Magnetic Resonance and Electron Paramagnetic Resonance Study
Giorgio Zoppellaro, Espen Harbitz, Ravinder Kaur, Amy A. Ensign, Kara L. Bren, K. Kristoffer Andersson
Journal of the American Chemical Society, **2008**, 130 (46), 15348-15360

Paper IV

Studies of Ferric Heme Proteins with Highly Anisotropic/Highly Axial Low Spin (S=1/2) Electron Paramagnetic Resonance Signals with bis-Histidine and Histidine-Methionine Axial Iron Coordination
Giorgio Zoppellaro, Kara L. Bren, Amy A. Ensign, Espen Harbitz, Ravinder Kaur, Hans-Petter Hersleth, Ulf Ryde, Lars Hederstedt, K. Kristoffer Andersson
Biopolymers, **2009**, 91 (12), 1064-1082

Publications not included in thesis

A comparative reactivity study of microperoxidases based on hemin, mesohemin and deuterohemin
Ekaterina S. Ryabova, Patrik Rydberg, Matthias Kolberg, Espen Harbitz, Anne-Laure Barra, Ulf Ryde, K. Kristoffer Andersson, Ebbe Nordlander
Journal of Inorganic Biochemistry, **2005**, 99 (3), 852-863

Reactive complexes in myoglobin and nitric oxide synthase
Hans-Petter Hersleth, Armelle Varnier, Espen Harbitz, Åsmund Kjendseth Røhr, Peter Paul Schmidt, Morten Sørlie, F. Henning Cederkvist, Stephane Marchal, Antonius C. F. Gorren, Bernd Mayer, Takeshi Uchida, Volker Schunemann, Teizo Kitagawa, Alfred X. Trautwein, Toru Shimizu, Reinhard Lang, Carl Henrik Gørbitz, K. Kristoffer Andersson
Inorganica Chimica Acta, **2008**, 361 (4), 831-843

Thermodynamic analysis of L-arginine and N-omega-hydroxyl-L-arginine binding to nitric oxide synthase
Henrik Zakariassen, F. Henning Cederkvist, Espen Harbitz, Toru Shimizu, Reinhard Lange, Bernd Mayer, Antonius C. F. Gorren, K. Kristoffer Andersson, Morten Sørlie
Biochimica et Biophysica Acta – Proteins and Proteomics, **2008**, 1784 (5), 806-810

1 Introduction

1.1 Metal ions in biology

Around 90 elements have been present throughout evolution, and about 30 of these are recognised as essential to some form of life (Kaim and Schwederski 1994; Lippard and Berg 1994; Emsley 2001). Half of these are non-metal elements, and include the key elements associated with life: carbon, nitrogen, oxygen, phosphorus and sulphur. These elements make up the bulk of atoms in biology, but equally important for life are metals found in different amounts in all cells (Finney and O'Halloran 2003; Waldron, Rutherford et al. 2009). The S-block elements (Na^+, K^+, Mg^{2+} and Ca^{2+}) are the most abundant metal ions in biological systems. They participate in a wide range of processes, from the triggering of biochemical reactions by being vital for enzyme catalysis, to electrostatic stabilisation of biomolecules. Calcium also has an important role in bones and shells. The S-block metals in biological systems occur mostly as mono- or di-valent ions in solution or in coordination with anionic biomolecules (like in Mg^{2+}-ATP). One important exception is chlorophyll, the primary photoreceptor in photosynthesis, where magnesium is bound in a cyclic tetrapyrrole (Fischer 1937). The “trace” metals found among the D-block elements serve a great variety of roles in the chemistry of life. The ability to form several stable redox states makes them ideally suited for catalysis. The importance of metals in biology can be recognised by the fact that 47 % of enzymes with known 3D structure require metal ions, with 41 % containing metal ions at their catalytic centre (Waldron, Rutherford et al. 2009). The name trace elements is a bit misleading, as the concentrations of these metals are up to several orders of magnitude higher inside the cells relative to the concentration in typical growth conditions (Finney and O'Halloran 2003). As these metals participate in cytotoxic processes like the generation of reactive oxygen species, the concentration of free metal ions within a cell is tightly controlled (Finney and O'Halloran 2003; Hentze, Muckenthaler et al. 2004; Valko, Morris et al. 2005).

Iron is one of the most prevalent of the trace elements in our bodies and its presence has been known since the 18th century. The reason for this early discovery is the shear amount of iron needed in the organism. A grown up person normally contains roughly 4 grams of iron (Emsley 2001), and iron is essential in substantial amounts for most cellular organisms from

bacteria to mammals, with the exception of some anaerobic bacteria (Harrison and Arosio 1996). In biological systems iron is predominantly found in functional sites in proteins, such as iron-centres (containing 1 or 2 iron atoms), iron sulphur clusters or covalently bound in haem groups, or in iron storage proteins.

1.2 Haemoproteins

Haemoproteins are a large group of iron containing proteins where the iron is coordinated in a tetrapyrrole ring system consisting of four pyrrole rings linked by single atom bridges. There are several different haem groups found in nature, and they differ in the substituents pointing out from the pyrrole rings. These macrocyclic tetrapyrrole ring systems without the iron are called Porphyrins, after the Greek word *porphyra,* which means purple. With an iron in the middle of the ring system the porphyrin is called haem after the Greek word for blood, *Haima* (Figure 1).

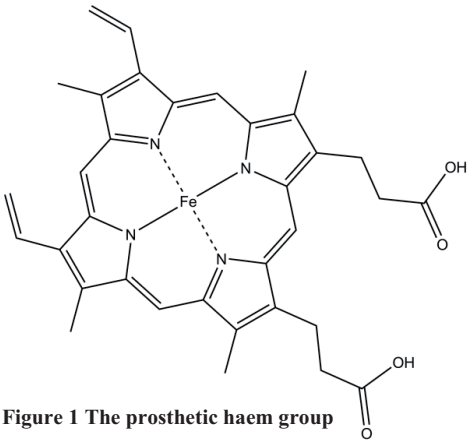

Figure 1 The prosthetic haem group (haem *b* / iron protoporphyrin IX)

Similar macrocyclic tetrapyrrolic ring systems coordinating other metals are found in nature. Chlorophyll, the green light absorbing molecule in photosynthesis, consists of a magnesium atom ligated in a porphyrin complex. Similarly, we find a cobalt tetrapyrrole in cobalamin (vitamin B_{12}) (Brink, Hodgkin et al. 1954; Hodgkin 1954) and a nickel tetrapyrrole in coenzyme F430 (Pfaltz, Jaun et al. 1982; Battersby 2000). Specialised enzyme systems, chelatases, exist to insert these metals into the tetrapyrroles (Minakami 1958; Walker and Willows 1997; Brindley, Raux et al. 2003).

Haemproteins are involved in a diverse range of biochemical processes. The PROMISE[1] database from 1999 (Degtyarenko, North et al. 1997; Degtyarenko, North et al. 1999) recognizes four functional classes:

1. Catalysis - Catalases, oxygenases and peroxidases
2. Electron transfer - Cytochromes
3. Oxygen transport and storage - Globins, e.g. haemoglobin and myoglobin
4. Nitric oxide transport - Nitrophorins

[1] The Prosthetic groups and Metal Ions in Protein Active Sites Database Version 2.0

More recently there have been found haemoproteins that act as sensor proteins (Rodgers 1999; Sasakura, Hirata et al. 2002) and haem binding proteins that act as transcriptional regulators (Kaasik and Lee 2004; Kitanishi, Igarashi et al. 2008). The haem based sensor proteins can have altered catalytic activity upon binding of diatomic ligands, like NO binding in guanylate cyclase (Denninger and Marletta 1999), or they can be transcriptional regulators, like the oxygen sensing proteins FixL, which restrict expression of specific genes under hypoxic conditions (Gong, Hao et al. 1998); and the CO binding CooA, which regulates the expression of *coo* genes associated with CO-dependent growth (Aono, Nakajima et al. 1996).

The research on haem containing proteins can be dated back to the 18th century when Vincenzo Menghini (1704-1759) was able to show that the red blood cells contained considerable amounts of iron while the plasma did not (Severinghaus, Astrup et al. 1998). The iron was detected by burning blood, and observing that the ashes were attracted by a magnet (Windsor and Rodway 2007). The prosthetic nature of the haem ligand was determined by Jöns Jacob Berzelius (1779-1848) who was able to split the red material in blood into a protein component and a coloured component containing iron oxide (Berzelius 1806-1808). The chemical composition of this coloured component was determined by Johannes Mulder (1802-1880), who also demonstrated that it binds oxygen (Severinghaus, Astrup et al. 1998). In 1862 this pigment was renamed “haemoglobin” by Felix Hoppe-Seyler (1825-1895) who was able to crystallize the pigment, and described its optical spectrum (Hoppe 1862).

In the 18th century, observations suggested that the iron containing pigment was not a single entity. Boerhaave had already in 1771 observed the pigment in muscle, and noticed that it stayed in the tissue after all the blood was washed away (Boerhaave 1771; Gunther 1921). These two pigments were originally both named haemoglobin, only distinguished by the words blood haemoglobin and muscle haemoglobin (the latter was renamed myoglobin in 1921 (Gunther 1921)). In 1884-1886 C.A. MacMunn described “colouring matters” from fresh tissue of vertebrates, which showed a near relationship to haemoglobin, but he also observed some differences. A significant difference was that “the pigmented portion cannot as in the case of haemoglobin be separated from the proteid constituent” (MacMunn 1887). The absorption spectrum MacMunn observed in his tissue preparations included an absorption band, which was not found in the spectrum of blood haemoglobin as observed by Hoppe-Seyler or muscle haemoglobin as observed by Wilhelm Friedrich

Kühne (Kühne 1865). MacMunn named the observed pigment in muscle Myohaematin, and when it was observed in other tissues Histohaematins. His findings were not recognized by his contemporaries and even rejected as haemoglobin contamination by Hoppe-Seyler (Hoppe-Seyler 1890).

1.3 Cytochromes

The respiratory pigments C.A. MacMunn had observed in 1884-86 were hardly mentioned in the scientific literature until they was rediscovered in 1925 by David Keilin (1887-1963). Keilin introduced the word cytochrome, merely signifying "cellular pigment" (Keilin 1925). Keilin found cytochromes in all animals he studied, in the 40 insect species he examined, in higher plants and in bacteria and yeast. He concluded that cytochrome "is one of the most widely distributed respiratory pigments".

Keilin observed, as MacMunn had reported, four absorption bands in the visible spectrum (Figure 2), which deviated only slightly between all of the species he had studied. These four bands were visible in the reduced state, but not in oxidised samples. He named them *a*, *b*, *c* and *d* after their position, and noticed that the *d*-band had several maxima.

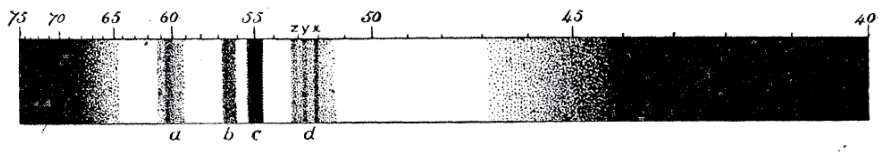

Figure 2 Keilin's absorption spectrum of cytochrome in a 0.65 mm slice of thoracic muscle of a bee (Keilin 1925).

Using various extraction methods, it was possible to get different "*hæmochromogen*" derivatives, which exhibited different absorption spectra. These extracts did not all contain the four absorption bands, and Keilin concluded that the cytochrome could be broken down into three distinct components. These components all had two distinct absorption bands, one not present in the other components, the α-band, and one (the β-band), which was similar in all three components (Figure 3). The β-bands from the three components together make up the observed *d*-band seen in Figure 2.

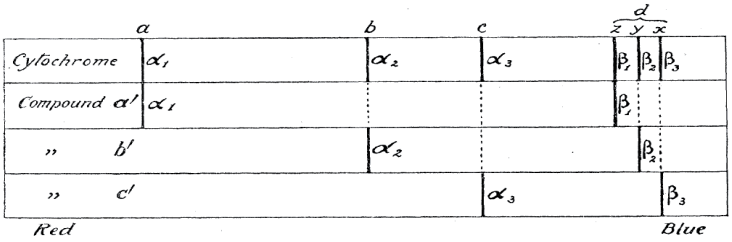

Figure 3 Keilin's diagram of the absorption peaks of cytochrome and the three "*hæmochromogen*" components derived from cytochrome. Figure from (Keilin 1925).

As Keilin's early experiments alluded to, the cytochrome reported is not a single entity. It is many different proteins with different prosthetic haem-groups. The different cytochrome components Keilin observed corresponds to proteins containing the three most common haem-groups, which have been named after the localization of their α-absorption bands.

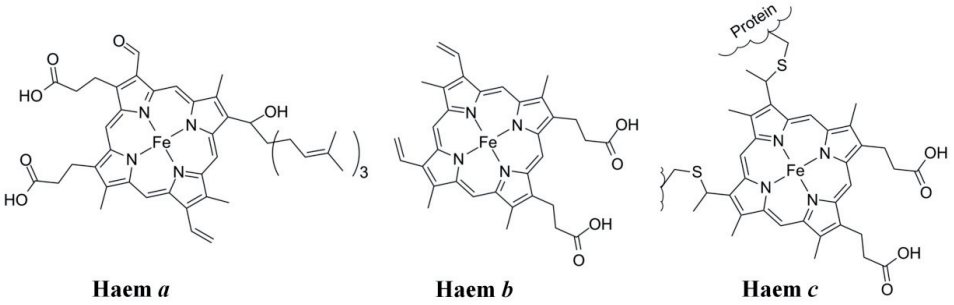

Figure 4 The chemical structure of the haem groups contained in cytochromes *a*, *b* and *c*.

The haem groups are redox active molecules, where the iron can reversibly alternate between the ferrous (Fe^{2+}) and ferric (Fe^{3+}) oxidation state, making them capable of transporting electrons between different chemical processes in the cell. The most common haem groups are shown in Figure 4. The haem groups differ in the substituents on the porphyrin ring. Several other haem groups are found, mainly in bacterial species, which have other substituents, and even partly saturated porphyrin rings (e.g. haem *d*) (Timkovich, Cork et al. 1985; Allen, Barker et al. 2005).

Cytochromes can be defined as electron transport proteins having one or more haem groups. They are normally classified according to the type of haem group they contain (e.g. cytochrome *a*, cytochrome *b* and cytochrome *c*). A notable exception is cytochrome *f*, which contains a *c*-type haem (Martinez, Huang et al. 1994; Carrell, Schlarb et al. 1999; Kurisu, Zhang et al. 2003; Stroebel, Choquet et al. 2003; Alric, Pierre et al. 2005). Despite

the name, cytochromes P450 is not involved in electron transfer, but is a class of enzymes responsible for the oxidation of a wide range of substrates (Ravichandran, Boddupalli et al. 1993; Nelson, Koymans et al. 1996; Guengerich 2001; Denisov, Makris et al. 2005; Hersleth, Ryde et al. 2006). In oxygen activating enzymes like cytochromes P450, the iron reaches higher oxidation states (such as the high-valent intermediate Fe^{IV}=O) as part of the reaction cycle (Hersleth, Ryde et al. 2006).

1.4 Cytochromes *a*

Cytochrome *a* refers to electron transport proteins with haem *a* as prosthetic group. Haem *a* was first isolated in 1951 by Otto Heinrich Warburg (Warburg and Gewitz 1951) and is a redox cofactor unique to the cytochrome *c* oxidase (Morell, Barrett et al. 1961; Smythe and Caughey 1970; Caughey, Smythe et al. 1975).

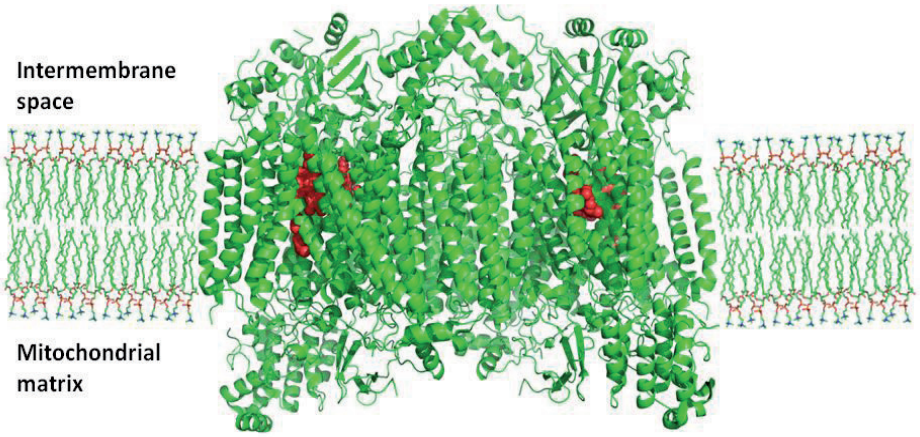

Figure 5 Cytochrome *c* oxidase from bovine heart. The oxidase complex is a homodimer, where each protomer consists of 13 subunits. The haems and O_2 are drawn in red. (Based on the x-ray structure PDBid 1V54 (Tsukihara, Shimokata et al. 2003).)

Cytochrome *c* oxidase (Figure 5) is the terminal complex in the respiratory chain, where electrons from aerobic metabolism reduce O_2 to water. In eukaryotes, cytochrome *c* oxidase contains two haem *a* (one low-spin and one high-spin), and two redox-active copper centres. The reason for the metabolically expensive haem *a* is not known, but might be associated with modulation of the haem binding affinity and reduction potential (Zhuang, Reddi et al. 2006). In bacterial species, other combinations of haem groups are

also found in terminal oxidases. These include the haem *a* precursor haem *o*, and haem *b*, *c* and *d* (Garciahorsman, Barquera et al. 1994). Figure 6 shows how molecular oxygen binds between a copper ion and haem *a* in cytochrome *c* oxidase. Cytochrome *c* oxidase is responsible for more than 90 % of the biological oxygen consumption on Earth (Babcock 1999). The oxygen reduction is associated with transmembrane proton translocation (Wikstrom 1977; Belevich, Verkhovsky et al. 2006; Branden, Gennis et al. 2006). In contrast to many monooxygenases, where activated oxygen can be released from the enzyme, oxygen reduction by cytochrome *c* oxidase does not release harmful oxygenous compounds in the cell (Babcock and Wikstrom 1992).

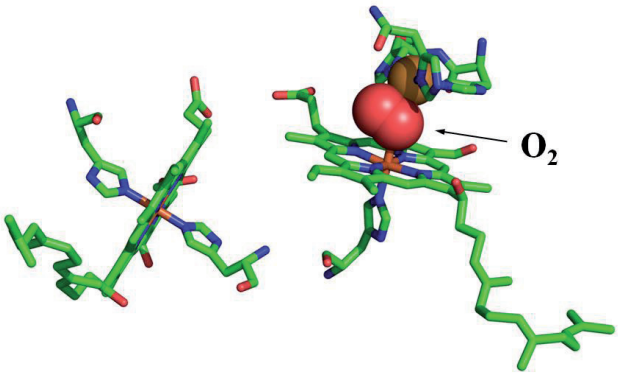

Figure 6 The oxygen binding site of cytochrome c oxidase. Molecular oxygen is bound between the iron in haem *a*, and a copper coordinated by histidines, before it is reduced in a stepwise manner to water. (Based on the x-ray structure 2Y69 (Kaila, Oksanen et al.)).

1.5 Cytochromes *b* and haem *b* proteins

Haem *b*, which is the prosthetic group of cytochromes *b* and many other haemoproteins, is the most abundant of the haem groups, and is found in all functional classes of haemoproteins. Haem *b* binds oxygen in the oxygen transport proteins myoglobin and haemoglobin; it is located in the active site of enzymes like cytochromes P450, catalase and nitric oxide synthase (NOS) (Hersleth, Ryde et al. 2006); it binds nitric oxide (NO) in nitrophorins present in the saliva of some bloodsucking insects (Champagne, Nussenzveig et al. 1995; Valenzuela, Walker et al. 1995; Weichsel, Andersen et al. 1998; Walker 2005; Yang, Knipp et al. 2009); and it has a functional role in the detection of oxygen or redox conditions (Kumar, Toledo et al. 2007; Cho, Cho et al. 2009; Kobayashi, Tanaka et al. 2010). A tumor suppressor protein has been identified as a cytochrome b561, with two

haem b groups (Berczi, Desmet et al. 2010). It is also found in several different electron transport proteins, which are thus named cytochromes *b*.

Cytochromes *b* are a diverse group of proteins, which serve a variety of functions in the cell. Some of the better known *b*-type cytochromes (as recognised by the PROMISE[2] database (Degtyarenko, North et al. 1997)) are described below.

1.5.1 Cytochromes *b* in the mitochondrial respiratory chain

In mammalian respiration *b*-type cytochromes are found as the terminal electron carrier in Complex II, and in two positions in Complex III (cytochrome bc_1) with distinct reduction potentials (Figure 7).

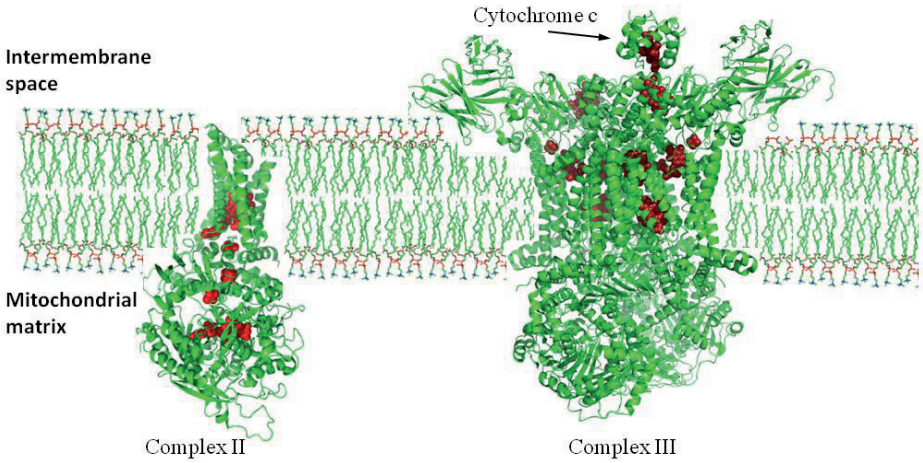

Figure 7 Complex II and Complex III of the eukaryotic respiratory chain. Redox active cofactors are coloured red. In the membrane domain of Complex II, we find a haem *b* that donates electrons to ubiquinone in the hydrophobic membrane layer to form ubiquinol. The ubiquinol is re-oxidized by haem b_H in the transmembrane part of Complex III, which sends the electron through haem b_L, an iron sulphur cluster, a haem c_1 and finally to the soluble cytochrome *c*. (The structure of Complex II is based on the x-ray structure PDBid 1YQ3 (Huang, Sun et al. 2006), and complex III is based on PDBid 1KYO (Lange and Hunte 2002).)

[2] The Prosthetic groups and Metal Ions in Protein Active Sites Database Version 2.0

The reduction potential of the haem groups in the respiratory chain increases incrementally to allow electron flow trough the different complexes and eventually to molecular oxygen (Wilson, Erecinsk.M et al. 1974). The electron flow is coupled to proton translocation across the membrane, which generates the proton motive force (PMF) needed for ATP synthesis. The iron in all three haem groups in Complexes II and III are coordinated by two histidine residues.

1.5.2 Cytochromes b_5

Cytochromes b_5 are a class of cytochromes *b* found in animals, plants, fungi and purple phototrophic bacteria. They were first observed by Cornelis F. Strittmatter, who found an unusual absorption band in a reduced sample of homogenized rat liver cells (Strittmatter and Ball 1954). Originally named cytochrome *m* because it was observed in microsomes, it is also found in the mitochondrial membrane (Altuve, Silchenko et al. 2001). The protein found in the microsomal and mitochondrial membranes has a hydrophobic N-terminal tail that anchors it to the membrane, and is found in all tissues (Figure 8). A differentially expressed, soluble splice variant that lacks the hydrophobic region is found in some tissues (Giordano and Steggles 1993).

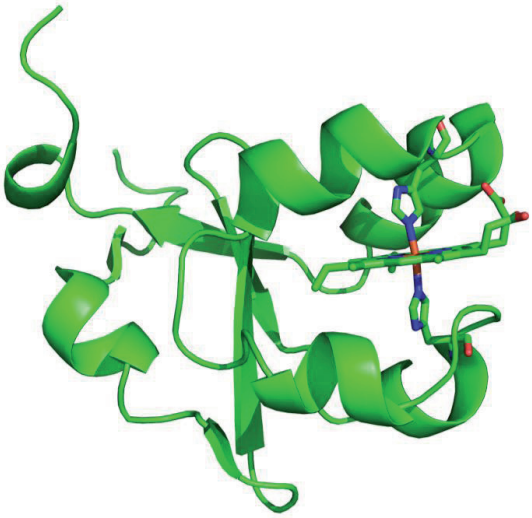

Figure 8 Soluble part of the outer mitochondrial membrane cytochrome b_5 from rat. The membrane attachment is achieved through a hydrophilic N-terminal tail. The haem iron is coordinated by two histidine residues. The structure is based on the x-ray structure PDBid 1ICC (Altuve, Silchenko et al. 2001).

In microsomes, cytochrome b_5 is a positive modifier of the cytochromes P450 monooxygenase reaction. The mechanism of this cooperativity is not fully elucidated, but suggested mechanisms involve the donation of the second electron in the reaction, or

decreasing the rate of uncoupling (Andersson 1980; Bonfils, Balny et al. 1981). Although named cytochrome, cytochromes P450 are an enzyme-family responsible for oxidising a large variety of substrates (Meunier, de Visser et al. 2004; Denisov, Makris et al. 2005). The reaction mechanism involves a two-electron reduction of molecular oxygen. Uncoupling of the P450 monooxygenase reaction between the activation of oxygen and the oxidation of substrate, leads to the release of superoxide or hydrogen peroxide (Degregorio, Sadeghi et al. 2011).

In addition to modifying the action of cytochromes P450, cytochromes b_5 is involved in the functioning of several fatty acid desaturases, Cr^{VI}-reductase and metmyoglobin and methaemoglobin reductases (Schenkman and Jansson 2003).

1.5.3 Cytochrome b_{562} and bacterioferritin

Cytochrome b_{562} is a monomeric, four-helix bundle protein found in the periplasm of *Escherichia coli* (Itagaki and Hager 1966). Although the function of this protein is not known, it has been extensively used as a model system for the study of haem ligation and protein folding (Arnesano, Banci et al. 2000; Garcia, Bruix et al. 2005). In contrast to most other cytochromes *b*, cytochrome b_{562} has a histidine and a methionine as the fifth and sixth haem ligand (Figure 9) (Arnesano, Banci et al. 1999). Despite differences in haem binding, axial ligand coordination and a small degree of sequence homology, cytochrome b_{562} and cytochrome *c*' are suggested to have a common molecular ancestor (Weber, Salemme et al. 1981).

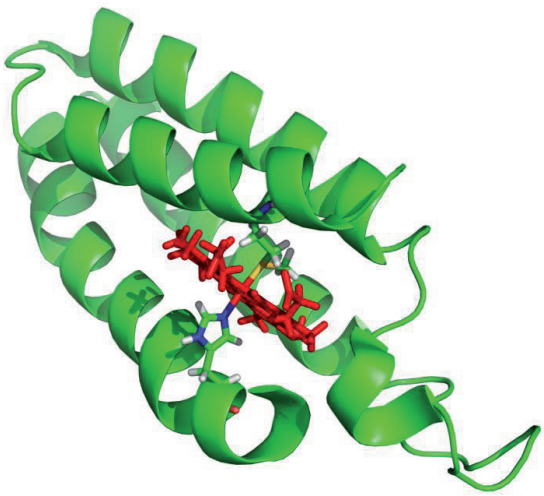

Figure 9 Cytochrome b_{562} from E. coli. The solvent accessible haem group is coordinated by histidine and methionine. (The figure is based on the NMR structure PDBid 1QPU (Arnesano, Banci et al. 1999).)

A similar four-helix fold as seen in cytochrome b_{562} is observed in the iron-storage protein bacterioferritin. Like ferritin, which is found in all domains of life, bacterioferritin assembles in a 24-mer cluster (Figure 10) to form a roughly spherical hollow structure with a cavity that can accommodate up to 4500 iron ions as an inorganic iron oxide complex (Harrison and Arosio 1996). Unlike ferritins, bacterioferritin incorporates 12 haems, bound between pairs of monomers of the protein. The haem irons are axially coordinated by two symmetry-related methionine residues, one from each subunit. Bis-methionine ligation of the haem iron is rare, and is only observed in bacterioferritins (Cheesman, Thomson et al. 1990), and in a haem transport protein believed to be involved in haem uptake in the bacteria *Streptococcus pyogenes* (Aranda, Worley et al. 2007). The haem in bacterioferritin facilitates the release of iron (Yasmin, Andrews et al. 2011), and may be involved in detoxification of iron and protection against reactive oxygen species (Carrondo 2003).

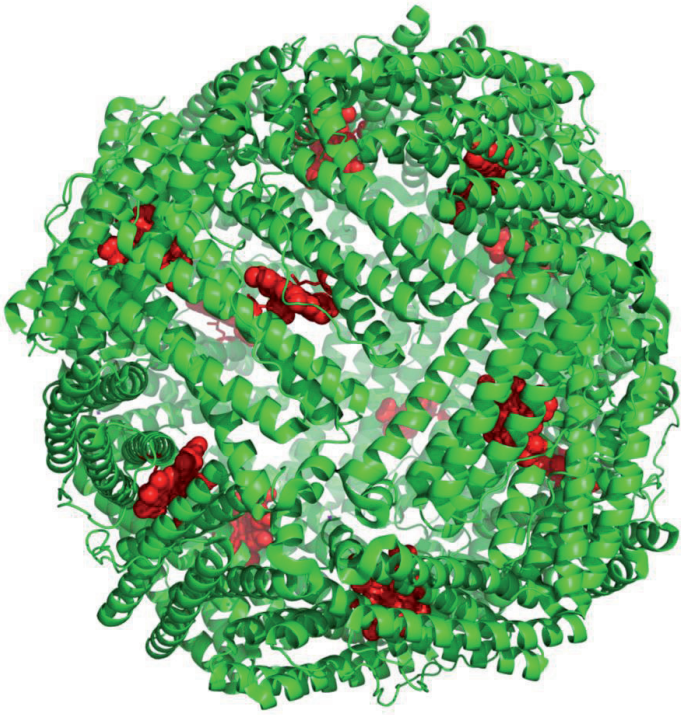

Figure 10 Bacterioferritin from *Pseudomonas aeruginosa* with haem groups and axial methionine ligands in red. (The figure is based on the x-ray structure PDBid 3IS8 (Weeratunga, Lovell et al. 2010).)

1.6 Cytochrome *c*

Cytochromes *c* are among the most studied proteins. This is probably due to the red colour common to haem proteins, making them easy to purify, and the high thermodynamic stability (Bertini, Cavallaro et al. 2006). The structure of the mitochondrial form of the protein was solved in 1977 (Swanson, Trus et al. 1977; Takano, Trus et al. 1977), followed by structures from several other sources.

In cytochromes *c*, the prosthetic haem group is covalently attached to the protein backbone by means of two (in rare examples one) thioether bonds. Three unique pathways are responsible for the incorporation of the haem in *c*-type cytochromes in different species (Kranz, Richard-Fogal et al. 2009). Despite the large machinery involved in cytochrome *c* biosynthesis, the formation of thioether linked haem in cytochrome *c* has also been observed in the absence of any biosynthetic machinery (Daltrop, Allen et al. 2002). The covalent attachment of the haem group to the protein backbone is the key characteristic of these proteins, and it is suggested that this is important for retaining the haem group outside the cytoplasm or in the mitochondrial intermembrane space (Wood 1983; Wood 1991). However, it may also be because the covalent haem attachment influences both haem reduction potential and ligand-iron interaction (Bowman and Bren 2008).

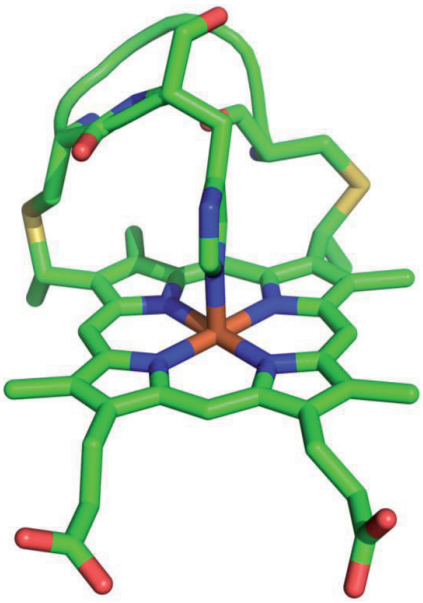

Figure 11 Haem c with the haem binding CXXCH motif. (Based on PDBid 1A56 (Timkovich, Bergmann et al. 1998).)

The haem binding motif, Cys-X-X-Cys-His, is highly conserved and provides the cysteine residues for the covalent attachment, as well as histidine axial ligand coordinating the haem iron (Figure 11). The histidine is structurally constrained, and the imidazole plane is aligned roughly along the haem α-γ meso axis (Zhong, Wen et al. 2004). The other axial iron ligand is most commonly methionine (e.g. mitochondrial cytochrome *c* (Bushnell, Louie et al. 1990), in the photosynthetic reaction centre (Lancaster and Michel 1996) and

soluble bacterial cytochromes (Salemme, Freer et al. 1973; Timkovich, Bergmann et al. 1998; Benini, Gonzalez et al. 2000)), but it can be histidine (e.g. cytochrome cd_1), the N-terminal amino group (cytochrome *f* in cytochrome b_6f in photosynthesis) (Carrell, Schlarb et al. 1999) or the iron can be five-coordinated like in cytochrome *c*' (Finzel, Weber et al. 1985).

1.6.1 Cytochromes *c* in eukaryotes

Cytochromes *c* are found in most eukaryotes, with the exception of some obligate parasites (e.g. *Encephalitozoon cuniculi* and *Trypanosoma brucei*) (Bertini, Cavallaro et al. 2006). There are two distinct types of cytochromes *c* found in eukaryotes; the small soluble mitochondrial cytochrome *c*, and the cytochrome c_1 domain in Complex III (Figure 12). Cytochrome c_1 is the terminal electron carrier in Complex III and donates one electron to the soluble cytochrome *c*, which is loosely bound to the outer surface of the inner mitochondrial membrane. The loose membrane attachment allows cytochrome *c* to shuttle between its binding partners in the membrane (Complex III and cytochrome *c* oxidase), and transferring electrons between them (Xia, Yu et al. 1997; Iwata, Lee et al. 1998; Lange and Hunte 2002).

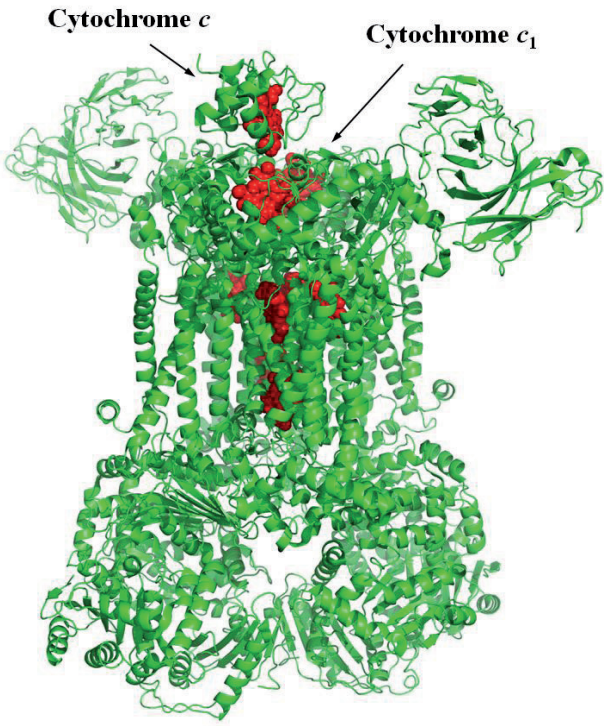

Figure 12 Complex III in association with mitochondrial cytochrome *c*. The distance between the haems in cytochrome c_1 and cytochrome c is 4.1 Å. The structure is based on PDBid 1KYO (Peitsch 1995; Lange and Hunte 2002).

In plants and photosynthetic bacteria, similar functions are performed by cytochrome b_6f and the copper containing protein plastocyanin. The cytochrome *f* domain is functionally analogous to cytochrome c_1. The haem in cytochrome *f* is a *c*-type haem covalently attached to the protein. An additional

atypical *c*-type haem is found in cytochrome b_6f, which is attached by one or two thioether linkage and has no axial amino acid ligand. This haem has been suggested to be involved in oxygenic photosynthesis (Martinez, Huang et al. 1994; Kurisu, Zhang et al. 2003; Stroebel, Choquet et al. 2003; Alric, Pierre et al. 2005).

In some eukaryotic organisms, isoforms of cytochrome *c* that can be expressed in a tissue specific manner is observed (Virbasius and Scarpulla 1988), or differentially expressed in response to oxygen concentration (Burke, Raitt et al. 1997). In plants, a cytochrome c_6 that can replace plastocyanin in the photosynthetic electron transport process has been observed (Gupta, He et al. 2002).

1.6.2 Cytochromes *c* in bacteria

Bacterial species contain in general a large variety of cytochromes *c*. In the genome of the alphaproteobacteria *Bradyrhizobium japonicum*, putatively 42 cytochrome *c* sequences have been detected, with a total of 62 cytochrome *c* domains. However, there also exist both bacterial and archaeal species that do not possess any cytochrome *c* domain (Bertini, Cavallaro et al. 2006). The large variation in the number of *c*-type cytochromes can be linked to the metabolic diversity of the bacteria. Purely fermentative bacteria do not need to possess a respiratory chain, and may not contain cytochromes. But frequently, a single species can possess a variety of possible electron transport chains (Buhler, Rossmann et al. 2010; Kawakami, Kuroki et al. 2010). This allows the bacterium to use a great variety of different molecules as electron donors and terminal electron acceptors in their metabolism. The number of different *c*-type cytochromes does, however, depend on whether the bacteria are Gram-positive or Gram-negative. Gram-negative bacteria have an outer membrane, and the *c*-type cytochromes involved in respiratory chains are found in the periplasmic space between the cell wall and the outer membrane. Gram-positive bacteria are observed to possess fewer *c*-type cytochromes than Gram-negative bacteria. Gram-positive bacteria do not possess an outer membrane, and the peptidoglycan layer surrounding the cell is not sufficient to retain small soluble proteins. The *c*-type cytochromes in Gram-positive bacteria thus need some sort of anchoring to the cell membrane. This anchoring can be achieved by linking one protein terminus to a lipophilic molecule, which can reside in the hydrophobic interior of the membrane, by addition of one or more transmembrane segments, or fusion with a membrane protein (Bertini, Cavallaro et al. 2006).

Historically, different naming systems have been employed for the *c*-type cytochromes according to their physical properties such as spectral features, redox potential or isoelectric point. In 1982, Richard Penry Ambler identified four major classes of *c*-type cytochromes based mainly on their amino acid sequence (Ambler 1982; Ambler 1991). More recently Ivano Bertini and co-workers have added classes to this list, based on their scanning of 188 genomes for cytochrome *c* domains. Their aim was to get a wide coverage of the possible roles of *c*-type cytochromes (Bertini, Cavallaro et al. 2006). The analysis of bacterial genomes revealed an astonishing variety in the number and types of *c*-type cytochromes encoded by different bacteria. *C*-type cytochromes are found as internal electron transfer domains in a great variety of oxidoreductases (e.g. terminal oxidases, bc_1 complexes, nitrite reductases, SoxAX complexes (for thiosulfate oxidation) and alcohol dehydrogenases), and as dedicated electron transfer proteins. The number of haem groups in each cytochrome can vary considerably, from the single haem found in most soluble *c*-type cytochromes (as in Figure 13) to long chains of haems, which can form "haem nanowires" (Pokkuluri, Londer et al. 2011). The axial ligation of the haem iron is most commonly bis-histidine, or methionine-histidine, with both being observed within the same protein. Recent analysis of bacterial genomes has revealed a vast number of genes that encode multihaem cytochromes *c*. The high number of multihaem cytochromes in bacteria has been correlated with their great respiratory flexibility (Londer, Giuliani et al. 2008; Alves, Paquete et al. 2011; Pokkuluri, Londer et al. 2011). Figure 14 shows a cytochrome *c* from *Geobacter*

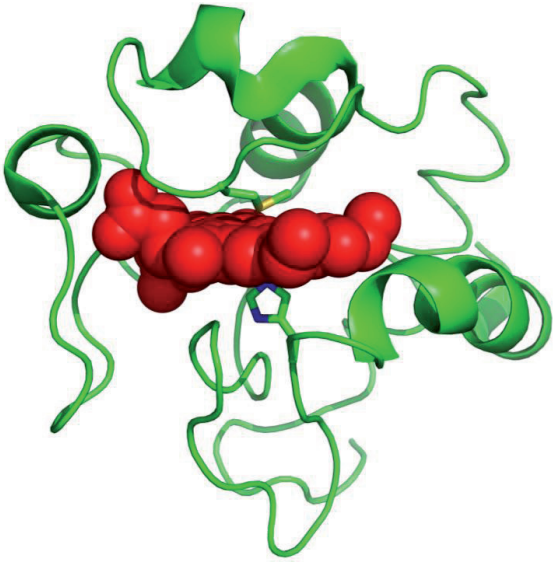

Figure 13 Cytochrome c_2 from *Rhodopseudomonas viridis*. Cytochrome c_2 is the closest bacterial homologue to the mitochondrial cytochrome *c*. The structure is based on PDBid 1CO6 (Sogabe and Miki 1995).

sulfurreducens containing 12 haem groups. This protein has 8 haems with bis-histidine ligation, and 4 haems with histidine-methionine ligation.

Multihaem assemblies are also found in intramolecular electron transfer in enzymes. The 24 haem enzyme hydroxylamine oxidoreductase from *Nitrosomonas europaea* consists of a homo-trimer, where each of the trimers contains eight haem groups (Igarashi, Moriyama et al. 1997). Seven of the haems are *c*-type haems, with bis-histidine ligation, and the last haem is an unusual haem P460. Despite the similarity in the haem ligation, the midpoint potentials of the *c*-type haems vary from -412 mV to +288 mV (Collins, Arciero et al. 1993). The structural arrangement of four of the haems in hydroxylamine oxidoreductase is strikingly similar to the haem arrangement in the tetrahaem cytochrome c_{554} from *Nitrosomonas europaea* suggesting an evolutionary relationship between these redox partners (Iverson, Arciero et al. 1998).

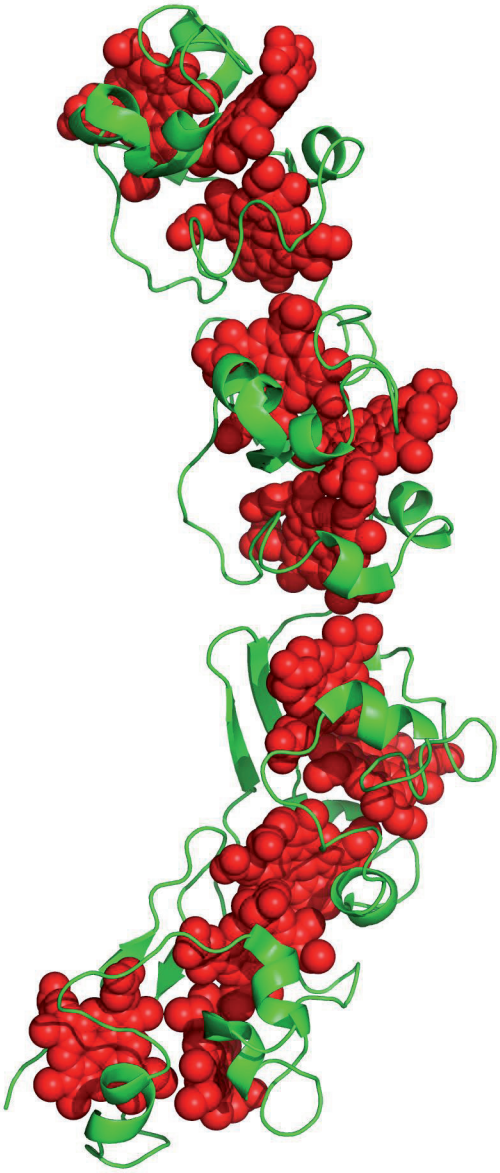

Figure 14 The dodecahaem cytochrome *c* from *Geobacter sulfurreducens*. The structure is based on PDBid 3OV0 (Pokkuluri, Londer et al. 2011).

1.7 Axial ligation in low-spin haems

In haemoproteins, the haem iron is always coordinated by the four nitrogen atoms in the tetrapyrrole ring system. In addition to this, the haem iron is normally coordinates by one or two amino acid ligands. The arrangement of axial ligands determines the energy levels of the *d*-orbitals on the iron, which determines the arrangement of the electrons in these orbitals (see Section 1.8.2). The state where the energy difference between the orbitals is sufficiently large to prevent the electrons from occupying the highest orbitals is called low-spin. In the low-spin configuration, the electrons pair together in the lower orbitals yielding a lower total spin.

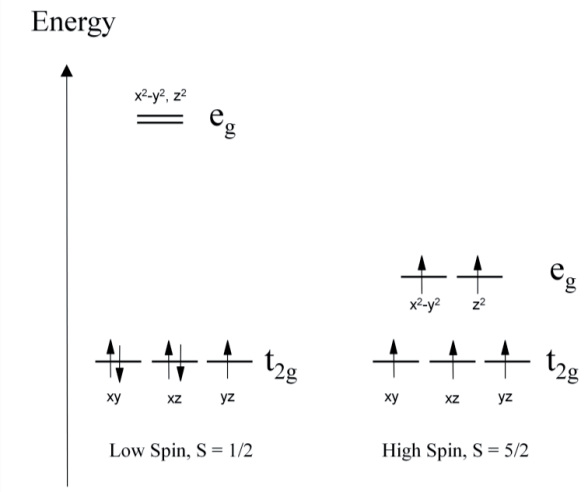

Figure 15 Energy diagram of the *d*-orbitals in low-spin and high-spin configuration of ferric haems. A large energy difference between the t_{2g} and e_g orbitals gives a state where the five electrons are all located in the t_{2g} orbitals, yielding a total spin of 1/2.

There are only four amino acids with side chains that have ligand field strengths sufficient to confine the haem to the low-spin state. These four amino acids are histidine, methionine, cysteine and lysine. Of the ten different combinations of these ligands, four has been observed in electron transfer proteins (Cheesman, Thomson et al. 1990). Bis-histidine ligation is commonly encountered in *b*-type cytochromes and partly in multihaem cytochromes *c*; methionine-histidine is common in *c*-type cytochromes and is found in cytochrome b_{562}; lysine-histidine is found in cytochrome *f*; and bis-methionine is found in bacterioferritin.

1.8 Spectroscopic analysis of haemoproteins

The spectroscopic techniques are all analytical methods that measure qualitatively and quantitatively the interaction of electromagnetic radiation with matter. The absorption of light by a sample probes the energy of an electronic transition, in which an electron is exited from a ground state to an exited state. Electromagnetic radiation is used to probe the energy difference between these two states. This energy difference reveals information about the molecule in question.

The most obvious information we can find by probing with electromagnetic radiation is colour. In coloured molecules, the energy difference between two states corresponds to electromagnetic radiation in the visible part of the spectrum. The foundation of spectroscopy is based on Isaac Newton's observation that sunlight that passed through a prism was refracted into "vivid and intense colours" (Newton 1671). The first direct observations of electronic transitions was the finding of specific absorption lines in the solar spectrum described by William Hyde Wollaston in 1802 (Wollaston 1802). Joseph

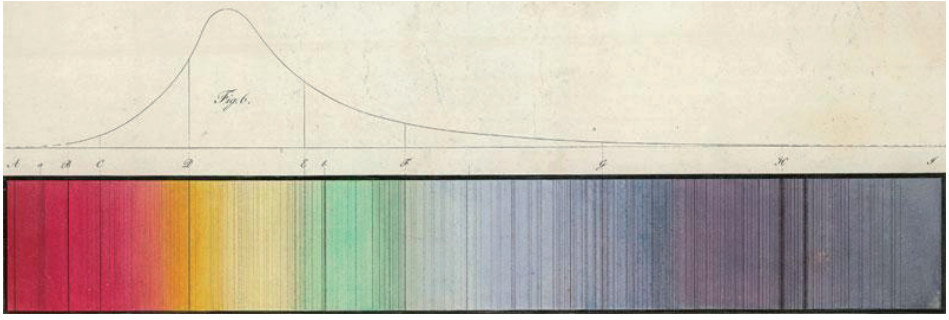

Figure 16 Fraunhofer's spectrum of the sun, with dark absorption bands. Copyright: Deutsches Museum, Munich.

Fraunhofer soon described several hundreds of dark lines appearing in the solar spectrum (Figure 16) (Fraunhofer 1817). The origin of these lines is absorption by chemical elements in the sun's atmosphere, but this was not understood before Robert Bunsen and Gustav Kirchhoff saw the same lines emitted from heated metals (Kirchhoff 1860). The observation by Bunsen and Kirchhoff, that different elements had distinct absorption bands, pioneered the use of spectroscopy in chemical analysis. Bunsen and Kirchhoff's spectroscope is shown in Figure 17.

Common to all spectroscopies is the key feature that the absorption or emission is plotted against the wavelength (or frequency/energy) of the radiation. Metal complexes, like the iron-containing haem group, frequently give rise to coloured compounds with absorption in the visible region of the electromagnetic spectrum. More spectroscopic information can be obtained by observing other parts of the electromagnetic spectrum like ultraviolet or infrared. Figure 18 shows how Keilin's absorption spectrum of "Cytochrome" relates to a quantitative spectrum of cytochrome *c*.

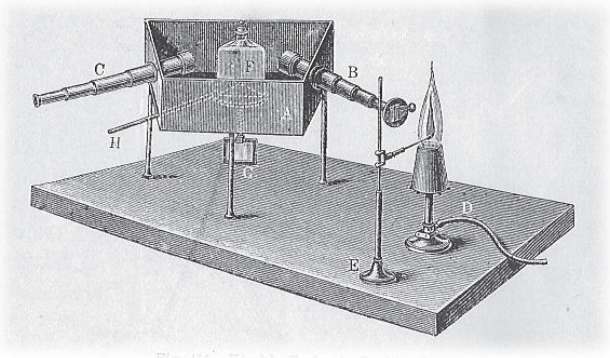

Figure 17 Bunsen and Kirchhoff's first spectroscope. Picture from ref (La Cour 1896) acquired through Wikimedia Commons.

Paramagnetic metal ions, like ferric iron (Fe(III)), will be influenced by external magnetic fields. This is a founding principle for Electron Paramagnetic Resonance (EPR) and Magnetic Circular Dichroism (MCD).

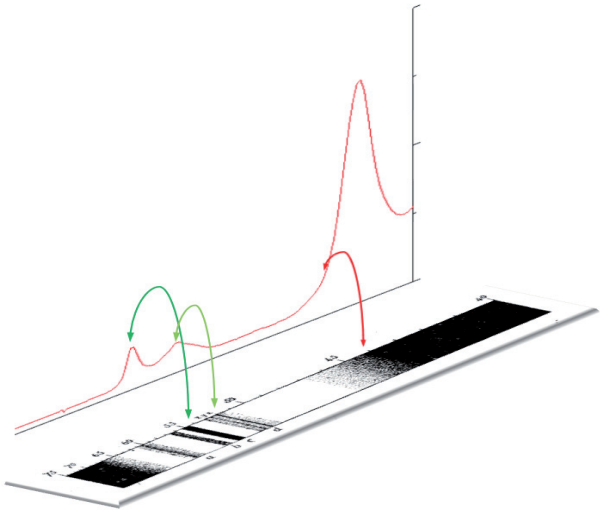

Figure 18 The relationship between a modern quantitative absorption spectrum of cytochrome *c* (spectrum taken from Paper 1), and Keilin's absorption spectrum from 1925. The visible spectrum showed here is bordered by the ultraviolet part of the spectrum to the right, and the infrared part of the spectrum at the left side of this figure. The characteristic Soret band of haemoproteins, observed just above 400 nm, was not distinguishable in the early spectra recorded by Keilin.

1.8.1 Electron paramagnetic resonance

Electron paramagnetic resonance (EPR) spectroscopy probes unpaired electrons in a sample. As the only unpaired electrons in proteins occur at metal ions or in free radical enzyme mechanisms, EPR is an excellent tool to study the chemically active part of a protein without interference from the protein backbone.

When placed in a magnetic field, the energy level of a free electron will depend on whether its spin is aligned with or against the magnetic field (Figure 19). The difference in energy between these two states can be probed by electromagnetic radiation. In the case of X-band EPR, the energy difference is probed by a fixed microwave at around 9-10 GHz and the magnetic field is varied (commonly from 0 to 0.6 T). The principle of EPR spectroscopy was first discovered by Evgeny Zavoisky (Zavoisky 1944; Zavoisky 1946) and Brebis Bleany (Bagguley, Bleaney et al. 1948; Bleaney and Penrose 1948), and has since been extensively applied to paramagnetic metal ions in biology (Miller and Brudvig 1991; Trautwein, Bill et al. 1991; Michel, Behr et al. 1998; Ohnishi 1998; Borbat, Costa-Filho et al. 2001).

The splitting of the energy levels is called the Zeeman Energy, and is given by equation 1, where β is the Bohr magneton, B_0 is the external magnetic field and *g* is the electron *g*-factor or spectroscopic splitting factor.

$$\Delta E = h\nu = g * \beta * B_0 \qquad 1$$

The *g*-factor is derived from the three dimensional Landé tensor. In a purely isotropic system, this tensor has equal components ($g_x = g_y = g_z$) in all directions and thus we get a single symmetric absorption band. In anisotropic systems the *g*-factor has different magnitude in each spatial direction, leading to a broad asymmetric absorption band. These features are not easily resolved in the absorption spectrum. By recording the first derivative of the EPR absorption spectrum, the three *g*-values can be resolved (Brudvig 1995).

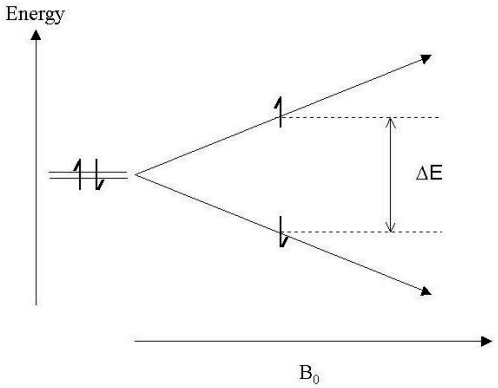

Figure 19 Schematic illustration of the splitting of the electron spin states in a magnetic field for spin 1/2 systems. When the splitting of the states, ΔE, equals the energy of the electromagnetic radiation, hν, we get an EPR absorption.

1.8.2 Electron paramagnetic resonance on cytochrome *c*

In haem groups involved in electron transfer, the natural oxidation states are ferrous, Fe^{2+}, and ferric, Fe^{3+}. The latter has five electrons in the *d*-orbitals, and can be studied by EPR spectroscopy. Depending on the energy differences between the *d*-orbitals (Figure 20), these electrons can either each occupy a different orbital, or together fill the three t_{2g} orbitals keeping the e_g orbitals unoccupied. In the first case the total spin is 5/2 and is called high-spin, and in the latter case the total spin is 1/2 and is called low-spin.

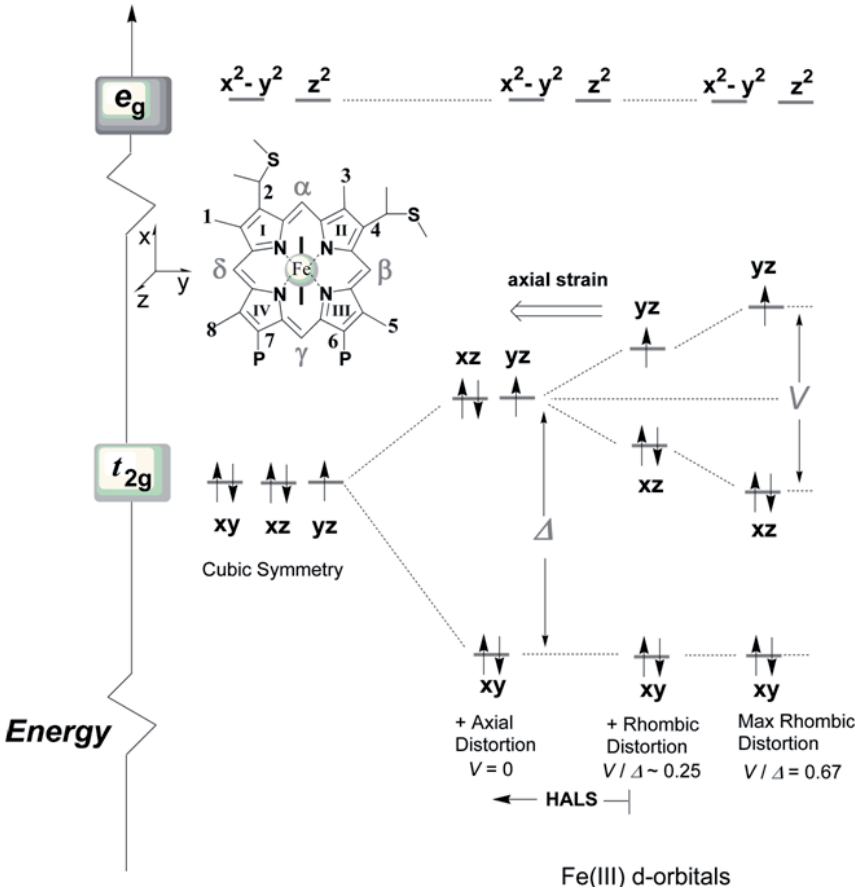

Figure 20 Energy diagram of the d-orbitals for low-spin ferric ions with $(d_{xy})^2(d_{xz})^2(d_{yz})^1$ orbital occupancy.

The low-spin form of ferric haem can exhibit different EPR signatures depending on the relative energy differences between the t_{2g} orbitals. The variation can be described by an axial distortion (Δ) of the octahedral ligand field along the axis perpendicular to the haem plane, and a rhombic distortion (V) in the plane of the haem. These factors can be calculated from the observed g-values in the EPR spectra using Equation **2** and **3**, thus linking the splitting of the orbital energy levels and the spin orbit coupling constant ξ, with observable factors.

$$\frac{V}{\xi} = \frac{E_{yz}}{\xi} - \frac{E_{xz}}{\xi} = \frac{g_{xx}}{g_{zz}+g_{yy}} + \frac{g_{yy}}{g_{zz}-g_{xx}} \qquad \mathbf{2}$$

$$\frac{\Delta}{\xi} = \frac{E_{yz}}{\xi} - \frac{E_{xy}}{\xi} - \frac{V}{2\xi} = \frac{g_{xx}}{g_{zz}+g_{yy}} + \frac{g_{zz}}{g_{yy}-g_{xx}} - \frac{V}{2\xi} \qquad \mathbf{3}$$

The first reliable EPR spectrum (according to Brautigan *et al*. (Brautigan, Feinberg et al. 1977)) on cytochrome *c* in frozen solution, was taken by Salmeen and Palmer in 1968 (Salmeen and Palmer 1968). The *g*-values they observed was 3.06, 2.24 and 1.24, and they also noted the absence of any paramagnetic absorption of the reduced form of cytochrome *c*. When recorded at cryogenic temperatures the EPR spectrum was observed to contain more features, and mammalian cytochromes *c* display up to four different low-spin EPR spectral forms that are in a pH dependent equilibrium (Theorell and Åkesson 1941; Brautigan, Feinberg et al. 1977). The high pH transition (Figure 21), which occurs at pK_a ~ 8.5 – 9.5, is known to involve conformational changes in the protein (Wilson 1996). In this conformational change, the axial methionine ligand is replaced by either one or the other of two lysine residues, giving rise to two new EPR forms with large g_{max} values at around 3.35 and 3.55 (Rosell, Ferrer et al. 1998).

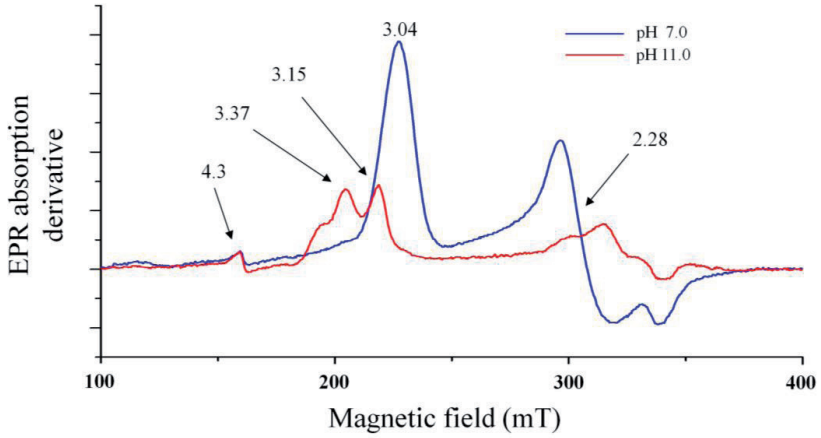

Figure 21 EPR spectra of horse heart cytochrome *c* at pH 7.0 and pH 11.0. At pH 7.0, the EPR lineshape is rhombic with *g*-values 3.04 and 2.28 (g_{min} not in spectrum). Above the alkaline transition the EPR spectrum probably consists of three different species. Two of the g_{max} values are resolved (g_{max} = 3.15 and g_{max} = 3.37) and a shoulder is observed on the low field (high *g*-value) side of the cytochromes g_{max} signal. The EPR feature with a *g*-value of 4.3 comes from mononuclear high-spin ferric iron in sites of low symmetry, and is commonly encountered in biological samples (Bou-Abdallah and Chasteen 2008).

1.8.3 The use of EPR for ligand assignment in cytochromes *c*

In the early seventies, Blumberg and Peisach analyzed a large number of ferric low-spin haem centres by EPR spectroscopy. They calculated the crystal field parameters, and plotted the rhombic to axial component (the "tetragonality"), Δ/ξ, versus the axial field strength (the "rhombicity"), V/Δ. They noticed that the data clustered into five regions named C, B, H, O and F (the letters are not related to the type of haem group). They found each of these regions to correspond to different axial ligation, with C having histidine-methionine ligation; B having two histidines with neutrally charged imidazole rings; H having two histidines where one, or both, imidazole rings are deprotonated; O having histidine and hydroxide ligation; and P having thiolate and a variety of alternative sixth ligands (Peisach, Blumberg et al. 1973). This correlation, known in the literature as the "truth diagram", has been used to predict the nature of the axial ligands in poorly characterised haem centres.

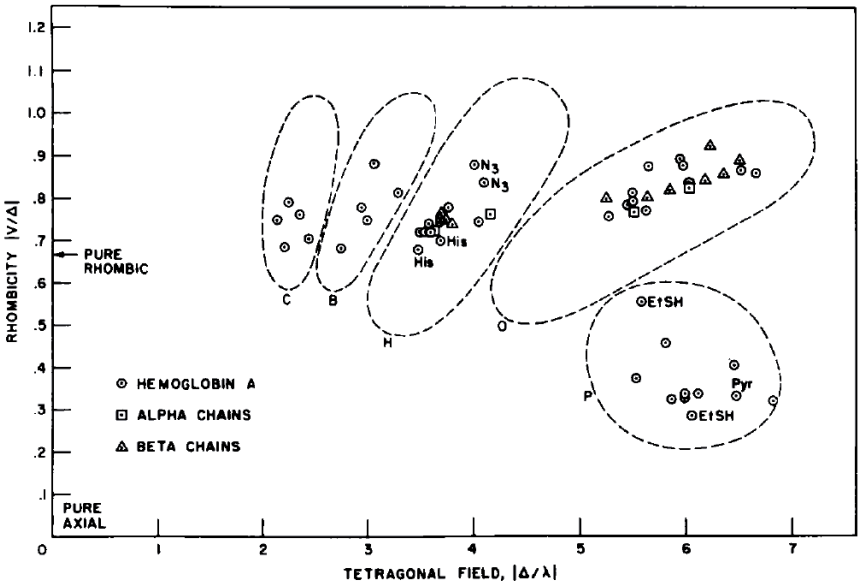

Figure 22 Blumberg and Peisach's "Truth Diagram" used to identify the axial ligands of low-spin ferrihaem proteins. The classification was based on analysis of the crystal field parameters obtained from the three *g*-values of the rhombic EPR spectra. Reprinted from reference (Peisach, Blumberg et al. 1973). Copyright 1971, American Chemical Society.

More recently, several cytochromes have been observed, both with histidine-methionine and histidine-histidine ligation, that exhibit single-feature low-spin EPR signals with $g_{max} \geq 3.2$ at very low temperatures (Orme-Johnson, Hansen and Beinert 1974; Brautigan, Feinberg et al. 1977; Siedow, Power et al. 1978; de Vries and Albracht 1979; Arciero, Peng et al. 1994; Desmet, Berczi et al. 2011). These "large g_{max}" EPR signals has been termed Type I ferrihaem , or Highly Anisotropic or Highly Axial Low Spin (HALS) EPR signals. The ligand field parameters of these are not easily calculated, as the other two *g*-values are poorly resolved. By *in silico* simulations of the EPR spectrum it is possible to obtain estimates for the last two g-values, and thus get an estimate of the ligand field parameters. For "large g_{max}"-systems, these ligand field parameters do not fit into the Blumberg-Peisach "truth diagrams" (Walker 2004; Zoppellaro, Bren et al. 2009).

This means that EPR alone is not sufficient for determination of the axial ligands in systems that exhibit ferric low-spin signals with a "large g_{max}" / HALS / Type I EPR spectrum. One useful spectroscopic approach is to combine EPR studies with near-infrared

magnetic circular dichroism (NIR-MCD) studies at low temperatures, as different combinations of axial ligands give rise to characteristic features in NIR-MCD spectra (Gadsby and Thomson 1990).

2 Aim of study

The use of EPR spectroscopy to elucidate reaction mechanisms and metal coordination has been employed for several decades. The key element has been the ability to specifically observe redox states of metal centres and free radicals by their characteristic EPR spectral features. Low-spin haems hava been found to exhibit two markedly different kinds of EPR spectra, namely the "large g_{max}" or HALS EPR spectra and rhombic EPR spectra. In haems with histidine-histidine ligation, there has been found a correlation between these types of EPR behaviour and the geometry of the histidines relative to each other .

In this study, we have investigated *c*-type cytochromes, where the haem iron has a histidine and a methionine residue as the fifth and sixth ligand. In this class of cytochromes both HALS and rhombic EPR spectra has been observed, but the reason for these differences is not understood. As EPR spectroscopy on these proteins only probes the unpaired electrons on the haem iron, the cause of the variation must be found in the immediate surroundings of the haem iron. By combining different spectroscopic techniques and comparing them with structural information, we have been trying to elucidate the relationship between the spectroscopic behaviour and the geometry of the haem axial ligands.

The first part of these studies has been to characterize cytochrome *c*-554 from the methane oxidizing bacteria *Methylosinus trichosporium* OB3b. This protein exhibits a HALS EPR signal, while cytochrome *c*-555 from another methane oxidizing bacteria, *Methylococcus capsulatus* Bath, exhibits a rhombic EPR signal.

The other part of these studies has been focused on comparative analysis of structure and spectroscopic features of small soluble c-type cytochromes from different bacteria. Using Mössbauer, NMR, EPR and visible spectroscopies we want to probe the electronic state of the haem iron. A part of this study is done by site-directed mutagenesis around the haem iron to elucidate the effect of different amino acid substitutions and their effect on the electronic properties of the haem centre and the axial geometries.

3 Summary of papers

3.1 Paper I

Cytochrome *c*-554 from *Methylosinus trichosporium* OB3b; a protein that belongs to the cytochrome c_2 family and exhibit a HALS-type EPR signal

Espen Harbitz, K. Kristoffer Andersson

PLoS One, **2011**, Vol. 6 (7), Article Number: e22014

In this paper, we describe the purification and spectroscopic properties of a hitherto uncharacterized *c*-type cytochrome from the methane oxidizing bacteria *Methylosinus trichosporium* OB3b. Mass spectroscopy and chemical haem cleavage were used to determine the molecular weight to be 12230 Da, and to confirm the presence of a single haem group in the protein. Edman degradation yielded two amino acid sequences containing a total of 68 amino acids. These sequences were Blasted against the genome sequence of *Methylosinus trichosporium* OB3b, and the full sequence including a signal sequence was identified.

Sequence alignments and homology modelling revealed a characteristic cytochrome *c* fold, and a high degree of structural homology with the cytochromes c_2. Cytochromes c_2 are the closest bacterial homologues to mitochondrial cytochrome *c*, and are known to mediate electron transfer between bc_1 complexes and cytochrome *c* oxidases during aerobic growth.

Cytochrome *c*-554 from *Methylosinus trichosporium* OB3b exhibits a HALS (Highly Anisotropic or Highly Axial Low Spin**)** signal as revealed by low temperature EPR spectroscopy. The ligand field parameters observed for cytochrome *c*-554 fits the observed pattern for other cytochromes with similar ligation and EPR behaviour.

Visible spectroscopy and circular dichroism were used to detect a methionine ligation of the haem iron. Extinction coefficients were calculated for the α-, β-, and γ (Soret) peaks in the visible spectrum of the cytochrome in the reduced and oxidized state.

3.2 Paper II

Low-Temperature EPR and Mössbauer Spectroscopy of Two Cytochromes with His-Met Axial Coordination Exhibiting HALS Signals

Giorgio Zoppellaro, Thomas Teschner, Espen Harbitz, Volker Schünemann, Solveig Karlsen, David M. Arciero, Stefano Ciurli, Alfred X. Trautwein, Alan B. Hooper, K. Kristoffer Andersson.

CHEMPHYSCHEM, 2006, Vol. 7 (6), 1258-1267

In this paper we have analyzed the electronic properties of cytochrome *c*-552 from *Nitrosomonas europaea* and cytochrome *c*-553 from *Bacillus pasteurii* by EPR and Mössbauer spectroscopy. These two proteins have similar ligation of the haem iron and they both exhibit HALS (Highly Anisotropic or Highly Axial Low Spin) EPR signals.

In addition to the HALS signal, there is, however, a minor rhombic component in these spectra that is in a pH dependent equilibrium with the HALS signal. In *Bacillus pasteurii* cytochrome *c*-553 the rhombic component accounts for 6% of the ferric haem at pH 6.2, but it is not visible to EPR spectroscopy at pH 7.4 or pH 8.2. In *Nitrosomonas europaea* cytochrome *c*-552, the rhombic component accounts for 25% of the ferric haem signal at pH 7.5.

Mössbauer spectroscopy of *Nitrosomonas europaea* cytochrome *c*-552 confirms the presence of two ferric species as well as a ferrous component not visible by EPR. Both EPR and Mössbauer is consistent with a $(d_{xy})^2(d_{xz})^2(d_{yz})^1$ electronic ground state, which is typical for Type I model haems.

3.3 Paper III

Modulation of the Ligand-Field Anisotropy in a Series of Ferric Low-Spin Cytochrome *c* Mutants derived from *Pseudomonas aeruginosa* Cytochrome *c*-551 and *Nitrosomonas europaea* Cytochrome *c*-552: A Nuclear Magnetic Resonance and Electron Paramagnetic Resonance Study

Giorgio Zoppellaro, Espen Harbitz, Ravinder Kaur, Amy A. Ensign, Kara L. Bren, K. Kristoffer Andersson

Journal of the American Chemical Society (2008), 130 (46), 15348-15360

In this paper we have studied cytochrome *c* from *Pseudomonas aeruginosa* (*Pa c*–551) and *Nitrosomonas europaea* (*Ne c*–552) by EPR and NMR spectroscopies. Point mutations were induced in a key residue (Asn64) near the methionine axial ligand that have a considerable impact on both haem ligand–field strength and in the methionine orientation and dynamics (fluxionality).

Ne c–552 has a ferric low-spin (S=1/2) EPR signal characterized by large *g* anisotropy with g_{max} at 3.34. In *Ne c*–552, deletion of Asn64 (*Ne*N64Δ) changes the haem ligand–field from more axial to rhombic and also hindered the methionine fluxionality present in the wild–type enzyme. In *Pa c*–551 (with g_{max} at 3.20), replacement of Asn64 with valine induces a decrease in the axial strain and changes the methionine configuration.

Other mutants, resulting in modifications in the length of the axial methionine-donating loop, did not give appreciable alterations of the original ligand field, but had an impact on methionine orientation, fluxionality and relaxation dynamics. Comparison of the electronic fingerprints of these proteins reveals a linear relationship between axial strain and average NMR haem methyl shifts, which stands, irrespective of the methionine orientation or dynamics. Thus, for these histidine-methionine axially coordinated ferric haems, the large g_{max} EPR signal does not represent a special case, as is observed for bis-histidine coordinated low-spin haems.

3.4 Paper IV

Studies of Ferric Heme Proteins with Highly Anisotropic/Highly Axial Low Spin (S=1/2) Electron Paramagnetic Resonance Signals with bis-Histidine and Histidine-Methionine Axial Iron Coordination

Giorgio Zoppellaro, Kara L. Bren, Amy A. Ensign, Espen Harbitz, Ravinder Kaur, Hans-Petter Hersleth, Ulf Ryde, Lars Hederstedt, K. Kristoffer Andersson

Biopolymers (2009), 91 (12), 1064-1082

This paper is a review of ferric haemoproteins with bis-histidine and histidine-methionine axial iron ligation that exhibit HALS (Highly Anisotropic or Highly Axial Low Spin) EPR signals. In both coordination environments, the haem core can exhibit ferric low-spin EPR signals with either rhombic or HALS signatures.

In bis-histidine coordinated haems, these EPR envelopes are related to the orientation of the histidine residues relative to each other. Parallel histidine planes result in a rhombic EPR signal, whereas perpendicular histidine planes result in a HALS signal. For ferric haems with histidine/methionine coordination, however, a similar clear-cut correlation between the structure of the haem and its ligands and the EPR envelopes is not found.

The ligand field present in bis-histidine systems can be made strong enough by the axial groups' structural arrangement to force the rhombicity to approach zero. This is the strong axial case, where g_{max} approaches 4 and g_{mid} and g_{min} go to zero, as described in Griffith and Taylor's theory (Griffith 1957; Griffith 1971; Taylor 1977). For histidine-methionine ligated low-spin haems, the larger covalency present in the S─Fe bond renders these systems at best highly anisotropic, with a high g_{max} much larger than g_{mid}, but not really axial.

4 Discussion

The usefulness of EPR spectroscopy in the study of metal-containing proteins is due to the selectivity of the method. By only observing unpaired electrons, EPR is a powerful tool for investigating paramagnetic metal ions and radicals in proteins, without any overlapping signals from the surrounding protein. The spectra observed can provide information on the immediate surroundings of the paramagnetic species, and has been used (in combination with other spectroscopic techniques) to elucidate the ligation of metal ions in biology. EPR can provide both information about the type of metal ligands and their geometry.

The overall goal has been to gain insight into the relationship between the EPR spectra exhibited by *c*-type cytochromes and the structure of the haem and its ligands. In the following part, I will summarize our studies of a cytochrome *c* from *Methylosinus trichosporium* OB3b that exhibit an unusual EPR behaviour (Paper I), and our work to understand the molecular origin of this EPR signal (Paper II & III). In our search for the structural basis that leads to this EPR signal, we have compared *c*-type cytochromes from several sources, made site-directed mutants around the EPR active haem iron, and used EPR, NMR, circular dichroism (CD) and Mössbauer spectroscopies.

4.1 Characterization of cytochrome *c*-554 from *Methylosinus trichosporium* OB3b

A cytochrome *c* has been purified from the methane oxidizing bacteria *Methylosinus trichosporium* Methylosinus trichosporium OB3b, which was grown in a medium with a copper concentration of 10 μM. Under these conditions, the membrane bound particulate methane monooxygenase is expressed (Semrau, DiSpirito et al. 2010). This cytochrome exhibits a ferric HALS (Highly Anisotropic or Highly Axial Low Spin) low-temperature EPR signal, with a typical HALS lineshape and a g_{max} value of 3.40. The EPR spectrum changes slightly with pH. MALDI-TOF mass spectroscopy has shown that this cytochrome has a molecular weight of 12 230 Da. Chemical cleavage of the thioether bonds linking the haem to the protein, combined with mass spectroscopy gave mass spectra consistent with only one haem group.

The α-absorption band of the ferrous form of the protein has an absorption maximum at 554 nm. This peak is commonly used to name *c*-type cytochromes. The ferric (oxidized) form of the protein shows a weak absorption band at 695 nm. Together with a peak at 730 nm in the circular dichroism spectrum this indicates a His / Met coordination of the haem iron. The sequence of the first 39 N-terminal amino acids and 27 C-terminal amino acids has been determined by Edman degradation.

4.1.1 Sequence alignments and homology modelling

The peptide sequences identified by Edman degradation have been used to identify related proteins using BLAST (Altschul, Madden et al. 1997). The most similar proteins found are *c*-type cytochromes from bacteria belonging to the phylum *Bradyrhizobiaceae*, in which *Methylosinus trichosporium* OB3b is included. The genome of *Methylosinus trichosporium* OB3b has recently been sequenced (Stein, Yoon et al. 2010). The sequenced peptide fragments were used to identify the full DNA sequence of cytochrome *c*-554 in the genome. In addition to the full amino acid sequence of the protein, this approach revealed a putative signal sequence indicating a periplasmic localization of cytochrome *c*-554.

Sequence alignment of the complete amino acid sequence against a protein structure database showed that ferrocytochrome c_2 from *Rhodopseudomonas viridis* has 56 (52%) identical residues, a total of 74 (69%) positive residues and no gaps in the alignment. This is the most similar protein where the three dimensional structure is solved (pdb-id: 1CO6) (Sogabe and Miki 1995). The structure of this protein was used as a template for modelling the structure of cytochrome *c*-554 from *Methylosinus trichosporium* OB3b using the SWISS-MODEL workspace (Peitsch 1995; Arnold, Bordoli et al. 2006; Kiefer, Arnold et al. 2009).

Homology modelling is based on mapping the amino acid residues of the target sequence onto the template structure. The prerequisite is that the template structure has a similar amino acid sequence, and that there are no insertions or deletions. As tertiary structure is better conserved than the amino acid sequence (Chothia and Lesk 1986; Kaczanowski and Zielenkiewicz 2010), proteins with similar amino acid sequences are expected to have highly similar structures.

4.2 Cytochrome *c*-554 belongs to the cytochrome c_2 family

Structural alignment using the homology model shows that cytochrome *c*-554 is highly similar to cytochromes c_2. The cytochrome c_2 family is the closest bacterial homologue to the mitochondrial cytochrome *c*. Cytochrome *c* from mitochondria has 30% identical residues with cytochrome *c*-554 from *Methylosinus trichosporium* OB3b, but the predicted tertiary structure is highly similar. This homology is not surprising, as the mitochondrion is believed to originate from a prehistoric relative of *Rickettsia prowazekii*, which, like *Methylosinus trichosporium* OB3b, is an alphaproteobacterium (Andersson, Zomorodipour et al. 1998). Like the mitochondrial cytochromes *c*, cytochromes c_2 are known to be membrane associated and to mediate electron transfer between bc_1 complexes and cytochrome *c* oxidases during aerobic growth (Bertini, Cavallaro et al. 2006). A similar role is possible for cytochrome *c*-554, as the high theoretical pI suggests a weak membrane association and the signal sequence suggests a periplasmic localisation, which is a common localisation for cytochromes *c* (Hooper and Dispirito 1985).

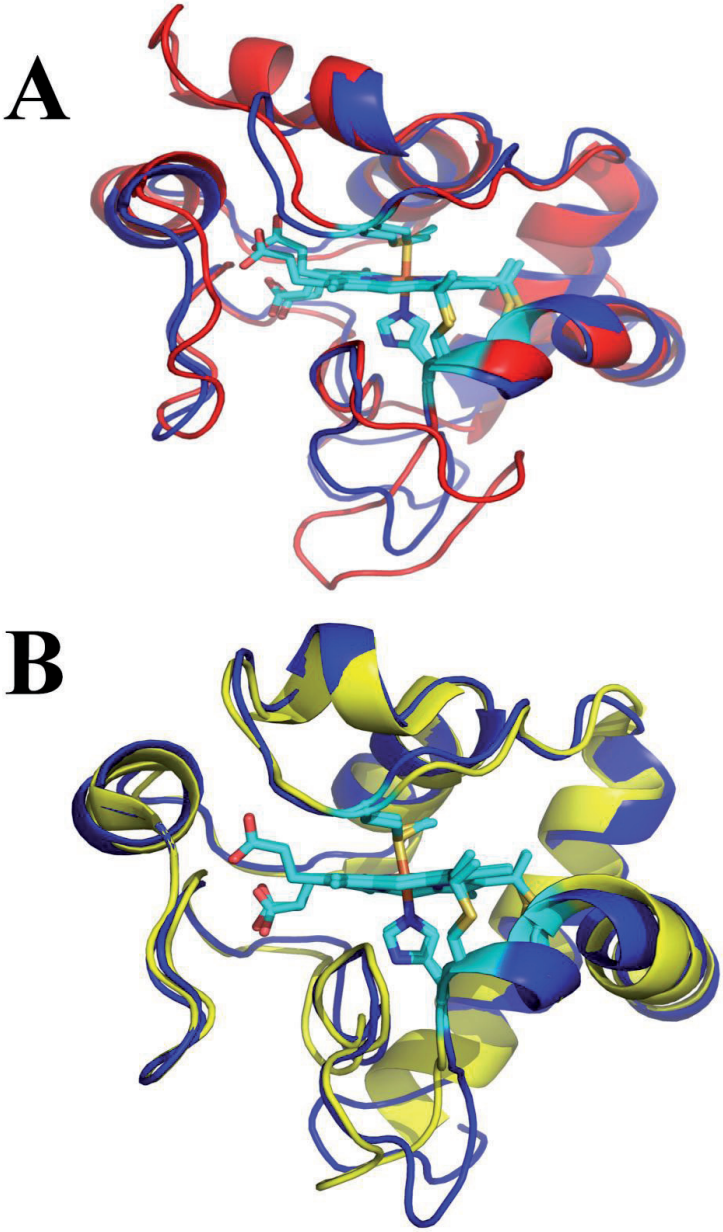

Figure 23 Structural alignment of the homology model of cytochrome *c*-554 from *Methylosinus trichosporium* OB3b (blue) and cytochrome *c* from horse heart (yellow). The highly similar tertiary structures place this cytochrome in the cytochrome c_2 family, which is the closest bacterial homologue to mitochondrial cytochrome *c* (Bertini, Cavallaro et al. 2006). The homology model of cytochrome *c*-554 from *Methylosinus trichosporium* OB3b was made using SWISS-MODEL, and the structure of cytochrome *c* from horse heart is based on PDBid 1HRC (Bushnell, Louie et al. 1990).

4.3 EPR spectroscopy on cytochrome *c*-554 from *Methylosinus trichosporium* OB3b

Cytochrome c-554 from *Methylosinus trichosporium* OB3b exhibits a ferric "large g_{max}" / HALS / Type I signal when subjected to low temperature EPR spectroscopy, with a g_{max} value of 3.40 (Figure 24). This signal differs from the rhombic EPR spectra observed in mitochondrial cytochromes *c* (Salmeen and Palmer 1968). We used a similar purification procedure to isolate a *c*-type cytochrome from the methane oxidising bacteria *Methylococcus capsulatus* Bath. Even if this bacterium and *Methylosinus trichosporium* OB3b have a similar methane metabolism, the cytochrome from *Methylococcus capsulatus* Bath exhibits a typical rhombic EPR spectrum. The biological role of these proteins is not certain, and they might be involved in different metabolic processes in their respective cells.

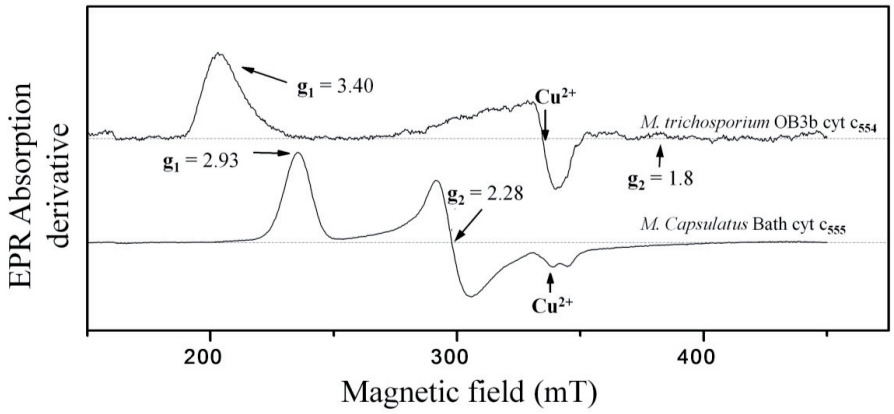

Figure 24 EPR spectra of cytochrome *c*-554 from *Methylosinus trichosporium* OB3b, and cytochrome *c*-555 from *Methylococcus capsulatus* Bath. The EPR spectrum of cytochrome *c*-554 from *Methylosinus trichosporium* OB3b has a HALS signal with a g_{max} value of 3.40, the other two g-values are not clearly resolved. Cytochrome *c*-555 from *Methylococcus capsulatus* Bath exhibits a rhombic EPR signal similar to what is observed for horse heart cytochrome *c*. Figure adapted from Paper I.

Because of the nature of the very broad HALS EPR signal, direct assignment of all three g-values is generally not possible. The microwave absorption amplitude decays slowly and extends to high magnetic fields resulting in a weak slope, and hence small amplitudes in

the 1st derivative spectrum. We simulated the EPR spectrum of cytochrome *c*-554 from *Methylosinus trichosporium* OB3b, and found that the spectrum is best fit with $g_y = 1.8$. The g_x-value was too broad for any meaningful simulation, and was calculated to be 1.1 using the equation $g_z^2 + g_y^2 + g_x^2 = 16$ (Griffith 1971; Taylor 1977; de Vries and Albracht 1979). It should be noticed that this sum of squares can be lower in systems with a fairly pure $(d_{xz},d_{yz})^4(d_{xy})^1$ ground state (Walker 1999), so the g-values at high field should be taken with caution. Using the equations of Taylor, the crystal field parameters were calculated to be $V/\xi = 0.994$, $\Delta/\xi = 4.57$. This gives the rhombicity $V/\Delta = 0.22$ and $a^2 + b^2 + c^2 = 1.0006$, which is in the acceptable range demanded by this analysis (Taylor 1977). These are refined values compared to what we reported in our review article (Zoppellaro, Bren et al. 2009), but still fitting the observed trend in EPR behaviour we observe for *c*-type cytochromes with histidine-methionine ligation.

The EPR signal of cytochromes *c* are known to be dependent on pH (Brautigan, Feinberg et al. 1977). When we observe the EPR behaviour of cytochrome *c*-554 from *Methylosinus trichosporium* OB3b at pH 7.0 and 8.2, there is a shoulder on the high magnetic field side of the g_{max} peak at pH 7.0 (Figure 25 A). This heterogeneity hints to the presence of

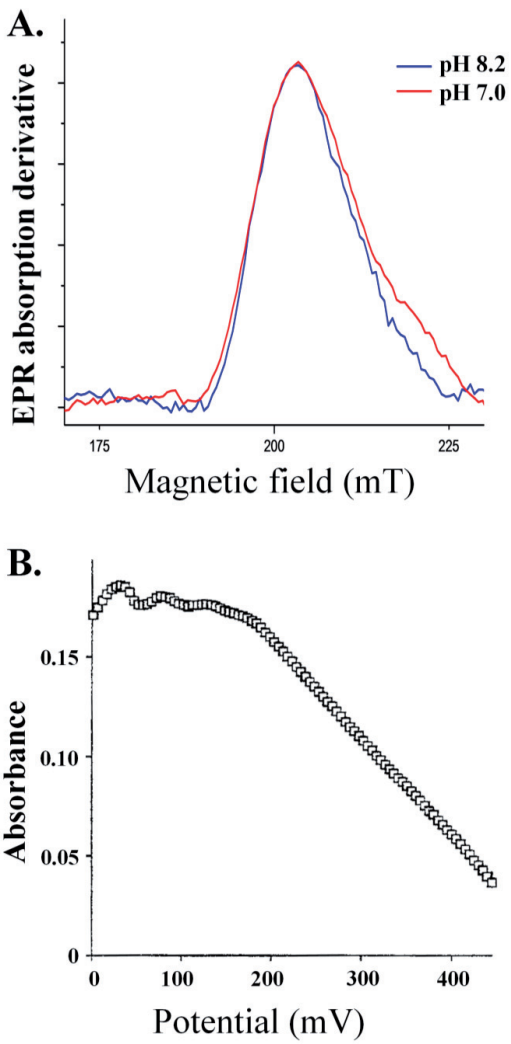

Figure 25 Heterogeneity of the electronic ground state. A. At pH 7.0, a shoulder is observed on the g_{max} peak compared to the spectrum recorded at pH 8.2 (unpublished results). B. Optical potentiometric titration reveals a redox potential higher than 200 mV, but could not be fit with a one-electron Nernst plot (Fauchald 2000).

more than one electronic state.

A preliminary optical potentiometric titration has been performed in Professor Alan B. Hooper's laboratory (University of Minnesota) to determine the redox potential of cytochrome *c*-554 (Collins, Arciero et al. 1993; Arciero, Hooper et al. 1994). This analysis was performed at pH 7.0, and resulted in an absorbance versus potential plot that could not be fit with a one-electron Nernst plot (Figure 25 B) (Fauchald 2000). The midpoint redox potential is higher than 200 mV, but was not accurately determined because of the heterogeneity of the spectral changes.

The heterogeneity in the spectropotentiometric behaviour and the shoulder in the EPR signal observed at pH 7.0 suggest the presence of more than one electronic configuration in the population of cytochrome *c*-554 molecules.

4.4 Mössbauer analysis of the electronic ground state

Several *c*-type cytochromes with histidine-methionine haem ligation that exhibit "large g_{max}" / HALS EPR signals have been observed to have heterogeneous EPR spectra. We have analyzed the electronic properties of cytochrome *c*-552 from *Nitrosomonas europaea* and cytochrome *c*-553 from *Bacillus pasteurii* by EPR spectroscopy over the pH range from 6.2 to 8.2. The electronic ground state of cytochrome *c*-552 has also been studied by Mössbauer spectroscopy (Paper II).

The g_{max}–peak in the EPR spectra of these proteins was observed to broaden in a pH dependent manner. This broadening can be rationalised by the presence of two low-spin species with different EPR behaviour. The EPR spectra can be simulated as a mixture of a "large g_{max}" / HALS signal and a rhombic EPR signal (Figure 26). The relative proportions of these species vary with pH. In *Bacillus pasteurii* cytochrome *c*-553, the rhombic component accounted for 6% of the ferric haem at pH 6.2, but it is not visible at pH 7.4 or pH 8.2. In *Nitrosomonas europaea* cytochrome *c*-552, the rhombic component accounted for 25% of the ferric haem signal at pH 7.5 (Paper II).

Cytochrome *c*-552 from *Nitrosomonas europaea* have been isolated from bacteria grown in a ^{57}Fe enriched medium in Professor Alan B. Hooper's laboratory (University of Minnesota). ^{57}Fe enrichment is a prerequisite for Mössbauer spectroscopy. The Mössbauer spectra of *Nitrosomonas europaea* cytochrome *c*-552 confirm the presence of two ferric species, as well as a ferrous component not visible by EPR. Both EPR and Mössbauer spectra are consistent with a $(d_{xy})^2(d_{xz}, d_{yz})^3$ electronic ground state, which is typical for Type I model haems. The Mössbauer parameters of the ferrous (reduced) cytochrome *c*-552 from *Nitrosomonas europaea* closely resemble the normal reduced horse heart cytochrome *c*, indicating that there are no large differences between the ferrous form of cytochromes exhibiting HALS or rhombic EPR signals (Paper II).

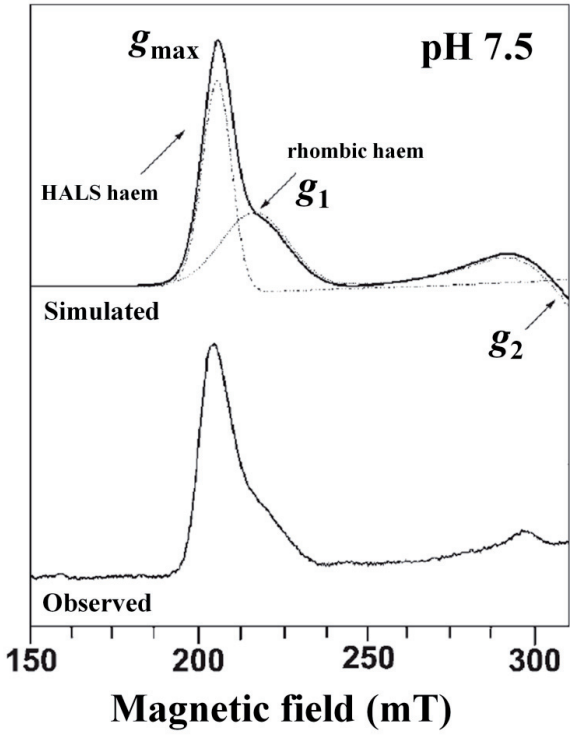

Figure 26 Simulation of the EPR signal of cytochrome c552 from Nitrosomonas europaea at pH 7.5. The simulation shows that the spectrum can be described as a mixture of two components. The rhombic component has a g_{max} of 3.18. Figure adapted from Paper II (Zoppellaro, Teschner et al. 2006).

4.5 Fluxionality of the methionine side-chain

The haem axial methionine is coordinated to the haem iron via a dative bond from the sulphur atom. This binding makes the sulphur a chiral centre, and the terminal methyl group can attach to the sulphur can in two different conformations. In 2004, Zhong *et al*. reported from NMR studies in solution that the methyl group could fluctuate between these two states in *Hydrogenobacter termophilus* (Zhong, Wen et al. 2004). A single amino acid

substitution was found to suppress this fluctuation and lock the methyl group in a single conformation (Wen and Bren 2005).

In the two highly similar cytochromes, cytochrome *c*-551 from *Pseudomonas aeruginosa* (Pa *c*–551) and cytochrome *c*-552 from *Nitrosomonas europaea* (Ne *c*–552), different methionine fluxionality was observed by Wen *et al.* (Wen and Bren 2005). In Ne *c*–552, the methionine displayed fluxional behaviour, whereas in Pa *c*–551 the methionine was locked in one position (Figure 27). Axial methionine fluxionality can be induced by substituting the haem pocket residue Asn64 with Gln (Wen and Bren 2005).

We used site-directed mutagenesis to examine the effect of different amino acids around the haem axial methionine in these two cytochromes (Paper III). Point mutations induced in a key residue (Asn64) near the methionine axial ligand had a considerable impact on both haem ligand–field strength and the methionine orientation and dynamics (fluxionality). In Ne *c*–552, deletion of Asn64 changed the haem ligand–field from more axial to rhombic and also hindered the methionine fluxionality present in the wild–type enzyme. In Pa *c*–551, replacement of Asn64 with Val induced a decrease in the axial strain and changed the methionine configuration.

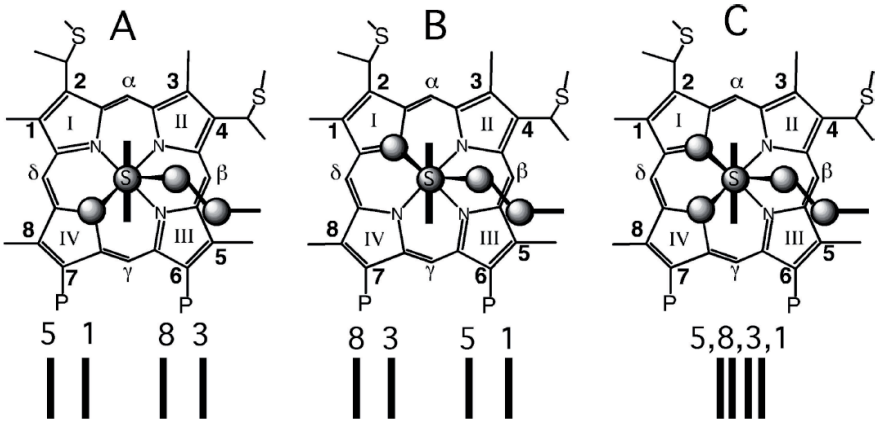

Figure 27 Axial methionine orientation and corresponding haem methyl paramagnetic ^{1}H NMR chemical shift patterns in cytochromes *c*. A. Methionine orientation observed in Pa *c*-551. B. Methionine orientation in mitochondrial cytochrome *c*. C. Illustration of methionine fluxionality with the methyl group sampling the two conformations shown in panels A and B. Ne c-552 shows such a condensed methyl shift pattern. Figure taken from Paper III (Zoppellaro, Harbitz et al. 2008).

Other mutants, resulting in modifications in the length of the axial methionine-donating loop, did not give appreciable alterations of the original ligand field, but had an impact on methionine orientation, fluxionality and relaxation dynamics (Paper III). This excludes a direct relationship between the axial strain as observed by EPR spectroscopy and the conformation of the axial methionine.

The four methyl substituents on the haem group experience the paramagnetic haem iron. For low-spin haems, the NMR chemical shift pattern of these four methyl substituents is paramagnetically shifted and is observed at higher ppm values (8-35 ppm). These methyl shifts is observed to be "fingerprints" of the conformation of the methionine (figure 27). Even though we do not see any direct relationship between the methionine conformational behaviour and the axial strain observed by EPR, we observe a linear relationship between axial strain and average NMR haem methyl shifts. This stands irrespective of the methionine orientation or dynamics (Paper III).

.

4.6 The "large g_{max}"/ HALS EPR signal

The "large g_{max}" / HALS / Type I EPR signal has been observed in cytochromes with both bis-histidine, histidine-amine and histidine-methionine coordination of the haem iron. The main characteristic of these signals is a g-value higher than 3.3 (Taylor 1977; de Vries and Albracht 1979; Salerno 1984; Walker 1999).

Both HALS and rhombic EPR behaviour is observed in bis-histidine and histidine-methionine ligated haem irons. As EPR spectroscopy probes the electrons around the haem iron, the origin of the observed differences must arise from differences in the environment around this iron. The relationship between the structural arrangement of the haem axial ligands and the EPR spectrum has been extensively studied in bis-histidine ligated haem model compounds (Walker, Huynh et al. 1986; Yatsunyk, Carducci et al. 2003; Walker 2004). The "large g_{max}" / HALS EPR signal is correlated with perpendicular alignment of the histidine ligand planes, and parallel axial ligand orientation gives rise to rhombic EPR spectra. The change between the "large g_{max}" / HALS and the rhombic spectral type appears to be at ~57±3-5º with continuous change in the g_{max}-value upon continuous change of the angle between the axial histidine ligand planes (Yatsunyk, Dawson et al. 2006). Structural information about proteins containing bis-histidine ligated haem groups is in agreement with the correlation between the g_{max} value and the relative orientation of the histidines.

In histidine-methionine ligated haems, a similar correlation between structural features and EPR spectral type is not observed. Through comparisons of bacterial *c*-type cytochromes (wild-type and mutants), we see a gradual change in g_{max}-values and ligand field parameters from the pure rhombic to highly axial / anisotropic systems as seen in Figure 28 (Paper IV).

The bacterioferritins, which have bis-methionine ligation of the haem iron, exhibit a normal rhombic EPR spectrum. The *g*-values of bacterioferritin from *Pseudomonas aeruginosa* are 2.86, 2.32 and 1.48 (Cheesman, Kadir et al. 1992).

Bis-methionine and histidine-amine ligation are only rarely found in proteins. This might explain why only one EPR spectral type has been observed for these types of systems.

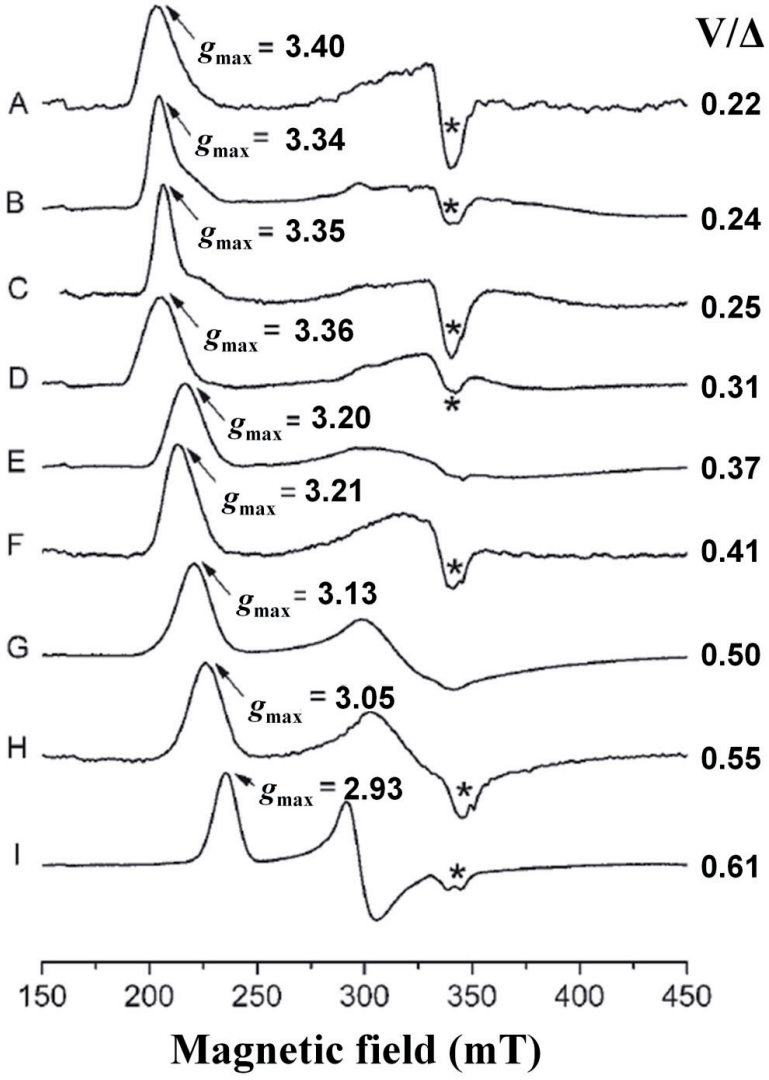

Figure 28 EPR spectra of bacterial *c*-type cytochromes (wild-type and mutants). A. *Methylosinus trichosporium* OB3b *c*–554, B. *Nitrosomonas europaea* Ne *c*–552, C. mutant NeV65Δ, D. *Bacillus pasteurii* *c*–553, E. *Pseudomonas aruginosa* *c*–551, F. mutant PaN64Q, G. mutant NeN64Δ, H. mutant PaN64V, I. *Methylococcus capsulatus* Bath *c*–554. The symbol Δ in the mutants indicate deletion of an amino acid. Figure adapted from Paper IV (Zoppellaro, Bren et al. 2009). The asterisks (*) indicates a signal arising from Cu^{2+} impurities. The symbol Δ indicates the axial term and V the rhombic term according to Griffith and Taylor's formalism (Griffith 1957; Taylor 1977).

4.7 Concluding remarks

To assess the orientation and dynamics of the axial groups and their impact on haem ligand-field anisotropy, NMR serves as an essential complement to EPR spectroscopy. This has revealed that there is no direct relationship between the axial strain as observed by EPR spectroscopy and the conformation of the axial methionine in histidine-methionine ligated haems. The lower electronegativity of the sulphur gives a larger degree of covalency in the Fe-S bond, and even small perturbations on the methionine side of the haem are apparently sufficient to trigger changes to the ligand field of the haem iron.

At present, it seems evident that the conformation of the axial ligands is not a dominant factor in determining the ligand field around the haem iron in histidine-methionine coordinated haems. Several factors contribute to the modulation of the ligand field strength, with subtle changes influencing the ligand field and / or axial ligand conformation. It thus appears that other factors, like second-sphere interactions and the planarity of the haem core, contribute to tuning the ligand field in a complicated manner. The pH dependent conversion between EPR spectral types observed in histidine-methionine ligated haems further complicates this picture. To elucidate the structural basis of the EPR spectral types observed in histidine-methionine ligated haem systems, complimentary methods for structure determination (X-ray crystallography) and determination of iron ligand distances (EXAFS) would be useful.

Cytochrome *c*-554 from *Methylosinus trichosporium* OB3b belongs to the class of cytochrome c_2. The homologue proteins mitochondrial cytochromes *c* and cytochrome c_2 from *Rhodobacter sphaeroides* are both membrane associated proteins, but despite an evolutionary relationship they show markedly different EPR behaviour (Salmeen and Palmer 1968; Drepper and Mathis 1997). Interestingly, the axial methionine ligand in the latter structure can be lost (Axelrod, Feher et al. 1994), as also suggested for horse heart cytochrome *c* at high pH (Brautigan, Feinberg et al. 1977; Hederstedt and Andersson 1986). This indicates, together with the fluxionality of the methionine ligand, that the methionine is loosely coordinated to the iron. Moreover, axial methionine seems more weakly coordinated to the haem than axial histidine. This can rationalise the observations that methionine ligation is more commonly found in covalently attached haems (*c*-type haems) and in haem-transport proteins, where a strong retention of the haem iron is not essential.

5 References

Allen, J. W. A., P. D. Barker, et al. (2005). "Why isn't 'standard' heme good enough for c-type and d(1)-type cytochromes?" Dalton Transactions(21): 3410-3418.

Alric, J., Y. Pierre, et al. (2005). "Spectral and redox characterization of the heme c(i) of the cytochrome b(6)f complex." Proceedings of the National Academy of Sciences of the United States of America **102**(44): 15860-15865.

Altschul, S. F., T. L. Madden, et al. (1997). "Gapped BLAST and PSI-BLAST: a new generation of protein database search programs." Nucleic Acids Research **25**(17): 3389-3402.

Altuve, A., S. Silchenko, et al. (2001). "Probing the differences between rat liver outer mitochondrial membrane cytochrome b(5) and microsomal cytochromes b(5)." Biochemistry **40**(32): 9469-9483.

Alves, A. S., C. M. Paquete, et al. (2011). "Exploration of the 'cytochromome' of Desulfuromonas acetoxidans, a marine bacterium capable of powering microbial fuel cells." Metallomics **3**(4): 349-353.

Ambler, R. P. (1982). The Structure an Classification of Cytochromes *c*. From Cyclotrons to Cytochromes. N. O. Kaplan, Robinson, A. New York, Academic Press**:** 263-280.

Ambler, R. P. (1991). "Sequence variability in bacterial cytochromes-c." Biochimica Et Biophysica Acta **1058**(1): 42-47.

Andersson, K. K. (1980). Cryobiochimie appliquée au fractionnement des protéines et à l'étude des intermédiaires réactionnels. Doctorat d'Université, Université des Sciences et Techniques du Languedoc (University Montpellier-II).

Andersson, S. G. E., A. Zomorodipour, et al. (1998). "The genome sequence of *Rickettsia prowazekii* and the origin of mitochondria." Nature **396**(6707): 133-140.

Aono, S., H. Nakajima, et al. (1996). "A novel heme protein that acts as a carbon monoxide-dependent transcriptional activator in Rhodospirillum rubrum." Biochemical and Biophysical Research Communications **228**(3): 752-756.

Aranda, R., C. E. Worley, et al. (2007). "Bis-methionyl coordination in the crystal structure of the heme-binding domain of the streptococcal cell surface protein shp." Journal of Molecular Biology **374**(2): 374-383.

Arciero, D. M., A. B. Hooper, et al. (1994). "Low-Volume Spectroelectrochemistry - an Anaerobic Optically Transparent Thin-Layer Electrode Cell and a Potentiostat Uv-Vis Spectrophotometer Interface for Computer-Controlled Data-Collection." Journal of Electroanalytical Chemistry **371**(1-2): 277-281.

Arciero, D. M., Q. Y. Peng, et al. (1994). "Identification of Axial Ligands of Cytochrome *c*(552) from *Nitrosomonas europaea*." FEBS Letters **342**(2): 217-220.

Arnesano, F., L. Banci, et al. (2000). "Structural consequences of b- to c-type heme conversion in oxidized Escherichia coli cytochrome b(562)." Biochemistry **39**(6): 1499-1514.

Arnesano, F., L. Banci, et al. (1999). "The solution structure of oxidized Escherichia coli cytochrome b(562)." Biochemistry **38**(27): 8657-8670.

Arnold, K., L. Bordoli, et al. (2006). "The SWISS-MODEL workspace: a web-based environment for protein structure homology modelling." Bioinformatics **22**(2): 195-201.

Axelrod, H. L., G. Feher, et al. (1994). "Crystallization and X-ray structure of cytochrome *c*2 from *Rhodobacter sphaeroides* in 3 Crystal Forms." Acta Crystallographica Section D-Biological Crystallography **50**: 596-602.

Babcock, G. T. (1999). "How oxygen is activated and reduced in respiration." Proceedings of the National Academy of Sciences **96**(23): 12971-12973.

Babcock, G. T. and M. Wikstrom (1992). "Oxygen activation and the conservation of energy in cell respiration." Nature **356**(6367): 301-309.

Bagguley, D. M. S., B. Bleaney, et al. (1948). "Paramagnetic Resonance in Salts of the Iron Group - A Preliminary Survey. 1. Theoretical Discussion." Proceedings of the Physical Society of London **61**(348): 542-550.

Battersby, A. R. (2000). "Tetrapyrroles: the pigments of life." Natural Product Reports **17**(6): 507-526.

Belevich, I., M. I. Verkhovsky, et al. (2006). "Proton-coupled electron transfer drives the proton pump of cytochrome *c* oxidase." Nature **440**(7085): 829-832.

Benini, S., A. Gonzalez, et al. (2000). "Crystal structure of oxidized *Bacillus pasteurii* cytochrome *c*(553) at 0.97-angstrom resolution." Biochemistry **39**(43): 13115-13126.

Berczi, A., F. Desmet, et al. (2010). "Spectral characterization of the recombinant mouse tumor suppressor 101F6 protein." European Biophysics Journal with Biophysics Letters **39**(8): 1129-1142.

Bertini, I., G. Cavallaro, et al. (2006). "Cytochrome *c*: Occurrence and functions." Chemical Reviews **106**(1): 90-115.

Berzelius, J. J. (1806-1808). Föreläsninger over Djurkemien. Stockholm, C. F. Marquard. **1-2**.

Bleaney, B. and R. P. Penrose (1948). "Paramagnetic Resonance at Low Temperatures in Chromic Alum." Proceedings of the Physical Society of London **60**(340): 395-396.

Boerhaave, H. (1771). Opera omnia Medica. Venetiis (Available trough Google Books).

Bonfils, C., C. Balny, et al. (1981). "Direct Evidence for Electron transfer from Ferrous Cytochrome b_5 to the Oxyferrous Intermediate of Liver Microsomal Cytochrome P450 LM2." Journal of Biological Chemistry **256**(18): 9457-9465.

Borbat, P. P., A. J. Costa-Filho, et al. (2001). "Electron spin resonance in studies of membranes and proteins." Science **291**(5502): 266-269.

Bou-Abdallah, F. and N. D. Chasteen (2008). "Spin concentration measurements of high-spin (g '=4.3) rhombic iron(III) ions in biological samples: theory and application." Journal of Biological Inorganic Chemistry **13**(1): 15-24.

Bowman, S. E. J. and K. L. Bren (2008). "The chemistry and biochemistry of heme *c*: functional bases for covalent attachment." Natural Product Reports **25**(6): 1118-1130.

Branden, G., R. B. Gennis, et al. (2006). "Transmembrane proton translocation by cytochrome c oxidase." Biochimica Et Biophysica Acta-Bioenergetics **1757**(8): 1052-1063.

Brautigan, D. L., B. A. Feinberg, et al. (1977). "Multiple Low-Spin Forms of Cytochrome c Ferrichrome - EPR Spectra of Various Eukaryotic and Prokaryotic Cytochromes c." Journal of Biological Chemistry **252**(2): 574-582.

Brindley, A. A., E. Raux, et al. (2003). "A story of chelatase evolution - Identification and characterization of a small 13-15-kda "ancestral" cobaltochelatase (CbiX(s)) in the archaea." Journal of Biological Chemistry **278**(25): 22388-22395.

Brink, C., D. C. Hodgkin, et al. (1954). "X-ray Crystallographic Evidence on the Structure of Vitamin B12 " Nature **174**(4443): 1169-1171.

Brudvig, G. W. (1995). "Electron paramagnetic resonance spectroscopy." Methods in Enzymology **246**: 536-554.

Buhler, D., R. Rossmann, et al. (2010). "Disparate Pathways for the Biogenesis of Cytochrome Oxidases in Bradyrhizobium japonicum." Journal of Biological Chemistry **285**(21): 15704-15713.

Burke, P. V., D. C. Raitt, et al. (1997). "Effects of oxygen concentration on the expression of cytochrome c and cytochrome c oxidase genes in yeast." Journal of Biological Chemistry **272**(23): 14705-14712.

Bushnell, G. W., G. V. Louie, et al. (1990). "High-Resolution 3-Dimentional Structure of Horse Heart Cytochrome *c*." Journal of Molecular Biology **214**(2): 585-595.

Carrell, C. J., B. G. Schlarb, et al. (1999). "Structure of the soluble domain of cytochrome *f* from the cyanobacterium *Phormidium laminosum*." Biochemistry **38**(30): 9590-9599.

Carrondo, M. A. (2003). "Ferritins, iron uptake and storage from the bacterioferritin viewpoint." Embo Journal **22**(9): 1959-1968.

Caughey, W. S., G. A. Smythe, et al. (1975). "Heme a of Cytochrome c Oxidase - Structure and Properties - Comparisons with Heme b, c, and s and Derivatives." Journal of Biological Chemistry **250**(19): 7602-7622.

Champagne, D. E., R. H. Nussenzveig, et al. (1995). "Purification, Partial Characterization, and Cloning of Nitric Oxide Carrying Heme Proteins (Nitrophorins) from Salivary Glands of the Bloodsucking Insect Rhodnius Prolixus." Journal of Biological Chemistry **270**(15): 8691-8695.

Cheesman, M. R., F. H. A. Kadir, et al. (1992). "EPR and Magnetic Circular-Didhroism Spectroscopic Characterization of Bacterioferritin from *Pseudomonas aeruginosa* and *Azotobacter vinelandii*." Biochemical Journal **286**: 361-367.

Cheesman, M. R., A. J. Thomson, et al. (1990). "Bis-Methionine Axial Ligation of Heme in Bacterioferritin from *Pseudomonas aeruginosa*." Nature **346**(6286): 771-773.

Cho, H. Y., H. J. Cho, et al. (2009). "Structural Insight into the Heme-based Redox Sensing by DosS from Mycobacterium tuberculosis." Journal of Biological Chemistry **284**(19): 13057-13067.

Chothia, C. and A. M. Lesk (1986). "The Relation between the Divergence of Sequence and structure in Proteins." Embo Journal **5**(4): 823-826.

Collins, M. J., D. M. Arciero, et al. (1993). "Optical Spectropotentiometric Resolution of the Hemes of Hydroxylamine Oxidoreductase - Heme Quantitation and Ph-Dependence of E(M)." Journal of Biological Chemistry **268**(20): 14655-14662.

Daltrop, O., J. W. A. Allen, et al. (2002). "In vitro formation of a c-type cytochrome." Proceedings of the National Academy of Sciences of the United States of America **99**(12): 7872-7876.

de Vries, S. and S. P. J. Albracht (1979). "Intensity of Highly Anisotropic Low-Spin Heme EPR Signals." Biochimica Et Biophysica Acta **546**(2): 334-340.

Degregorio, D., S. J. Sadeghi, et al. (2011). "Understanding uncoupling in the multiredox centre P450 3A4-BMR model system." Journal of Biological Inorganic Chemistry **16**(1): 109-116.

Degtyarenko, K. N., A. C. T. North, et al. (1997). "PROMISE: A new database of information on prosthetic centres and metal ions in protein active sites." Protein Engineering **10**(3): 183-186.

Degtyarenko, K. N., A. C. T. North, et al. (1999). "PROMISE: a database of bioinorganic motifs." Nucleic Acids Research **27**(1): 233-236.

Denisov, I. G., T. M. Makris, et al. (2005). "Structure and chemistry of cytochrome P450." Chemical Reviews **105**(6): 2253-2277.

Denninger, J. W. and M. A. Marletta (1999). "Guanylate cyclase and the .NO/cGMP signaling pathway." Biochimica Et Biophysica Acta-Bioenergetics **1411**(2-3): 334-350.

Desmet, F., A. Berczi, et al. (2011). "Axial ligation of the high-potential heme center in an Arabidopsis cytochrome b561." FEBS Letters **585**(3): 545-548.

Drepper, F. and P. Mathis (1997). "Structure and function of cytochrome *c*(2) in electron transfer complexes with the photosynthetic reaction center of *Rhodobacter sphaeroides*: Optical linear dichroism and EPR." Biochemistry **36**(6): 1428-1440.

Emsley, J. (2001). Nature's Building Blocks - An A-Z Guide to the Elements, Oxford University Press.

Fauchald, S. (2000). Preparative Isolation and Spectroscopical Characterization of a CO-binding *c*-type cytochrome and a novel *c*-type cytochrome from the methanotroph *Methylosinus trichosporium* OB3b. *Cand.Scient.*, University of Oslo.

Finney, L. A. and T. V. O'Halloran (2003). "Transition metal speciation in the cell: Insights from the chemistry of metal ion receptors." Science **300**(5621): 931-936.

Finzel, B. C., P. C. Weber, et al. (1985). "Structure of Ferricytochrome *c*' from *Rhodospirillum Molischianum* at 1.67 Å resolution." Journal of Molecular Biology **186**(3): 627-643.

Fischer, H. (1937). "Chlorophyll." Chemical Reviews **20**(1): 41-68.

Fraunhofer, J. (1817). "Bestimmung des Brechungs- und Farbenzerstreuungs-Vermögens verschiedener Glasarten." Denkschriften der koeniglichen Academie der Wissenschaften zu München **5**: 193 - 226.

Gadsby, P. M. A. and A. J. Thomson (1990). "Assignment of the Axial Ligands of Ferric Ions in Low Spin Hemoproteins by Near-Infrared Magnetic Circular Dichroism and Electron Paramagnetic Resonance Spectroscopy." Journal of the American Chemical Society **112**(13): 5003-5011.

Garcia, P., M. Bruix, et al. (2005). "Effects of heme on the structure of the denatured state and folding kinetics of cytochrome b(562)." Journal of Molecular Biology **346**(1): 331-344.

Garciahorsman, J. A., B. Barquera, et al. (1994). "The Superfamily of Heme-Copper Respiratory Oxidases." Journal of Bacteriology **176**(18): 5587-5600.

Giordano, S. J. and A. W. Steggles (1993). "Differential Expression of the Messenger-RNAs for the Soluble and Membrane-Bound Forms of Rabbit Cytochrome b5 " Biochimica Et Biophysica Acta **1172**(1-2): 95-100.

Gong, W. M., B. Hao, et al. (1998). "Structure of a biological oxygen sensor: A new mechanism for heme-driven signal transduction." Proceedings of the National Academy of Sciences of the United States of America **95**(26): 15177-15182.

Griffith, J. S. (1957). "Theory of Electron Resonance in Ferrihaemoglobin Azide." Nature **180**(4575): 30-31.

Griffith, J. S. (1971). "Theory of EPR in Low-Spin Ferric Haemoproteins." Molecular Physics **21**(1): 135-&.

Guengerich, F. P. (2001). "Common and uncommon cytochrome P450 reactions related to metabolism and chemical toxicity." Chemical Research in Toxicology **14**(6): 611-650.

Gunther, H. (1921). "Muscle pigment." Virchows Archiv Fur Pathologische Anatomie Und Physiologie Und Fur Klinische Medizin **230**: 146-178.

Gupta, R., Z. Y. He, et al. (2002). "Functional relationship of cytochrome c(6) and plastocyanin in Arabidopsis." Nature **417**(6888): 567-571.

Harrison, P. M. and P. Arosio (1996). "Ferritins: Molecular properties, iron storage function and cellular regulation." Biochimica Et Biophysica Acta-Bioenergetics **1275**(3): 161-203.

Hederstedt, L. and K. K. Andersson (1986). "Electron Paramagnetic Resonance Spectroscopy of *Bacillus subtilis* Cytochrome *b*-558 in *Escherichia coli* Membranes and in Succinate Dehydrogenase Complex from *Bacillus subtilis* Membranes." Journal of Bacteriology **167**(2): 735-739.

Hentze, M. W., M. U. Muckenthaler, et al. (2004). "Balancing acts: Molecular control of mammalian iron metabolism." Cell **117**(3): 285-297.

Hersleth, H. P., U. Ryde, et al. (2006). "Structures of the high-valent metal-ion haem-oxygen intermediates in peroxidases, oxygenases and catalases." Journal of Inorganic Biochemistry **100**(4): 460-476.

Hodgkin, D. (1954). "The X-ray Crystallographic Study of the Structure of Vitamin B12 " Acta Crystallographica **7**(10): 616-617.

Hooper, A. B. and A. A. Dispirito (1985). "In Bacteria Which Grows on Simple Reductants, Generation of a Proton Gradient Involves Extracytoplasmic Oxidation of Substrate." Microbiological Reviews **49**(2): 140-157.

Hoppe-Seyler, F. (1890). "Ueber Muskelfarbstoffe." Zeitschrift fur Physiologische Chemie **14**: 106-108.

Hoppe, F. (1862). "Ueber das Verhalten des Blutfarbstoffes im Spectrum des Sonnenlichtes." Virchows Archiv Fur Pathologische Anatomie **23**(1): 446-449.

Huang, L. S., G. Sun, et al. (2006). "3-Nitropropionic acid is a suicide inhibitor of mitochondrial respiration that, upon oxidation by Complex II, forms a covalent adduct with a catalytic base arginine in the active site of the enzyme." Journal of Biological Chemistry **281**(9): 5965-5972.

Igarashi, N., H. Moriyama, et al. (1997). "The 2.8 angstrom structure of hydroxylamine oxidoreductase from a nitrifying chemoautotrophic bacterium, *Nitrosomonas europaea*." Nature Structural Biology **4**(4): 276-284.

Itagaki, E. and L. P. Hager (1966). "Studies on Cytochrome b562 of Escherichia coli. I.Purification and Crystallization of Cytochrome b562 " Journal of Biological Chemistry **241**(16): 3687-&.

Iverson, T. M., D. M. Arciero, et al. (1998). "Heme packing motifs revealed by the crystal structure of the tetra-heme cytochrome c554 from Nitrosomonas europaea." Nature Structural Biology **5**(11): 1005-1012.

Iwata, S., J. W. Lee, et al. (1998). "Complete structure of the 11-subunit bovine mitochondrial cytochrome bc(1) complex." Science **281**(5373): 64-71.

Kaasik, K. and C. C. Lee (2004). "Reciprocal regulation of haem biosynthesis and the circadian clock in mammals." Nature **430**(6998): 467-471.

Kaczanowski, S. and P. Zielenkiewicz (2010). "Why similar protein sequences encode similar three-dimensional structures?" Theoretical Chemistry Accounts: Theory, Computation, and Modeling (Theoretica Chimica Acta) **125**(3): 643-650.

Kaila, V. R. I., E. Oksanen, et al. (2011) "A combined quantum chemical and crystallographic study on the oxidized binuclear center of cytochrome c oxidase." Biochimica et Biophysica Acta (BBA) - Bioenergetics **1807**(7), 769-778

Kaim, W. S., Birgitte (1994). Bioinorganic Chemistry: Inorganic Elemenst in the Chemistry of Life. Chichester, John Wiley & Sons.

Kawakami, T., M. Kuroki, et al. (2010). "Differential expression of multiple terminal oxidases for aerobic respiration in *Pseudomonas aeruginosa*." Environmental Microbiology **12**(6): 1399-1412.

Keilin, D. (1925). "On cytochrome, a respiratory pigment, common to animals, yeast, and higher plants." Proceedings of the Royal Society of London Series B-Containing Papers of a Biological Character **98**(690): 312-339.

Kiefer, F., K. Arnold, et al. (2009). "The SWISS-MODEL Repository and associated resources." Nucleic Acids Research **37**: 387-392.

Kirchhoff, G. B., Robert; (1860). "Chemische Analyse durch Spectralbeobachtungen." Annalen der Physik und der Chemie **110**: 161-189.

Kitanishi, K., J. Igarashi, et al. (2008). "Heme-binding characteristics of the isolated PAS-A domain of mouse Per2, a transcriptional regulatory factor associated with circadian rhythms." Biochemistry **47**(23): 6157-6168.

Kobayashi, K., A. Tanaka, et al. (2010). "Catalysis and oxygen binding of Ec DOS: a haem-based oxygen-sensor enzyme from Escherichia coli." Journal of Biochemistry **148**(6): 693-703.

Kranz, R. G., C. Richard-Fogal, et al. (2009). "Cytochrome c Biogenesis: Mechanisms for Covalent Modifications and Trafficking of Heme and for Heme-Iron Redox Control." Microbiology and Molecular Biology Reviews **73**(3): 510-+.

Kumar, A., J. C. Toledo, et al. (2007). "Mycobacterium tuberculosis DosS is a redox sensor and DosT is a hypoxia sensor." Proceedings of the National Academy of Sciences of the United States of America **104**(28): 11568-11573.

Kurisu, G., H. M. Zhang, et al. (2003). "Structure of the cytochrome b(6)f complex of oxygenic photosynthesis: Tuning the cavity." Science **302**(5647): 1009-1014.

Kühne, W. (1865). "Ueber den Farbstoff der Muskeln." Virchows Archiv Fur Pathologische Anatomie **33**: 79-94.

La Cour, P. A., Jacob (1896). Historisk Fysik. København, Det Nordiske Forlag.

Lancaster, C. R. D. and H. Michel (1996). "Three-dimensional structures of photosynthetic reaction centers." Photosynthesis Research **48**(1-2): 65-74.

Lange, C. and C. Hunte (2002). "Crystal structure of the yeast cytochrome bc(1) complex with its bound substrate cytochrome c." Proceedings of the National Academy of Sciences of the United States of America **99**(5): 2800-2805.

Lippard, S. J., J. M. Berg (1994). Principles of Bioinorganic Chemistry. Mill Valley, University Science Books.

Londer, Y. Y., S. E. Giuliani, et al. (2008). "Addressing Shewanella oneidensis "cytochromome": The first step towards high-throughput expression of cytochromes c." Protein Expression and Purification **62**(1): 128-137.

MacMunn, C. A. (1887). "Further observations on Myohaematin and the Histohaematins." The Journal of Physiology **8**(2): 51-116.

Martinez, S. E., D. Huang, et al. (1994). "Crystal Structure of Chloroplast Cytochrome *f* Reveals a Novel Cytochrome Fold and Unexpected Heme Ligation." Structure **2**(2): 95-105.

Meunier, B., S. P. de Visser, et al. (2004). "Mechanism of oxidation reactions catalyzed by cytochrome P450 enzymes." Chemical Reviews **104**(9): 3947-3980.

Michel, H., J. Behr, et al. (1998). "Cytochrome C oxidase: Structure and spectroscopy." Annual Review of Biophysics and Biomolecular Structure **27**: 329-356.

Miller, A. F. and G. W. Brudvig (1991). "A Guide to Electron Paramagnetic Resonance Spectroscopy of Photosystem II membranes." Biochimica Et Biophysica Acta **1056**(1): 1-18.

Minakami, S. (1958). "Biosynthesis of Heme and Hemeproteins in Tissue Cells - Iron Incorporation into Heme by preparations from Rat Liver " Journal of Biochemistry **45**(10): 833-844.

Morell, D. B., J. Barrett, et al. (1961). "Prosthetic Group of Cytochrome Oxidase. 1. Purification as Porphyrin a and Conversion into Haemin a " Biochemical Journal **78**(4): 793-&.

Nelson, D. R., L. Koymans, et al. (1996). "P450 superfamily: Update on new sequences, gene mapping, accession numbers and nomenclature." Pharmacogenetics **6**(1): 1-42.

Newton, I. (1671). "A Letter of Mr. Isaac Newton,..., Containing His New Theory about Light and Colors." Philosophical Transactions of the Royal Society of London **6**: 3075 - 3087.

Ohnishi, T. (1998). "Iron-sulfur clusters semiquinones in Complex I." Biochimica Et Biophysica Acta-Bioenergetics **1364**(2): 186-206.

Orme-Johnson, N. R., R. E. Hansen, H. Beinert (1974). "Electron Paramagnetic Resonance - Detectable Electron Acceptors in Beef Heart Mitochondria - Reduced Diphosphopyridine Nucleotide Ubiquinone Reductase Segment of Electron Transfer System " Journal of Biological Chemistry **249**(6): 1922-1927.

Peisach, J., W. E. Blumberg, et al. (1973). "Electron Paramagnetic Resonance Studies of Iron Porphin and Chlorin Systems." Annals of the New York Academy of Sciences **206**(OCT22): 310-327.

Peitsch, M. C. (1995). "Protein modeling by E-mail." Bio-Technology **13**(7): 658-660.

Pfaltz, A., B. Jaun, et al. (1982). "Factor-F430 from Metanogenic Bacteria - Structure of the Porphinoid Ligand System " Helvetica Chimica Acta **65**(3): 828-865.

Pokkuluri, P. R., Y. Y. Londer, et al. (2011). "Structure of a novel dodecaheme cytochrome c from Geobacter sulfurreducens reveals an extended 12 nm protein with interacting hemes." Journal of Structural Biology **174**(1): 223-233.

Ravichandran, K. G., S. S. Boddupalli, et al. (1993). "Crystal Structure of Hemoprotein Domian of P450BM-3, A Prototype for Microsomal P450's." Science **261**(5122): 731-736.

Rodgers, K. R. (1999). "Heme-based sensors in biological systems." Current Opinion in Chemical Biology **3**(2): 158-167.

Rosell, F. I., J. C. Ferrer, et al. (1998). "Proton-linked protein conformational switching: Definition of the alkaline conformational transition of yeast iso-1-ferricytochrome c." Journal of the American Chemical Society **120**(44): 11234-11245.

Salemme, F. R., S. T. Freer, et al. (1973). "Structure of Oxidized Cytochrome c_2 of *Rhodospirillum rubrum*." Journal of Biological Chemistry **248**(11): 3910-3921.

Salerno, J. C. (1984). "Cytochrome Electron Spin resonance Line Shapes, Ligand Field, and Components Stoichiometry in Ubiquinol Cytochrome *c* Oxidoreductase." Journal of Biological Chemistry **259**(4): 2331-2336.

Salmeen, I. and G. Palmer (1968). "Electron Paramagnetic resonance of Beef Heart Ferricytochrome c." Journal of Chemical Physics **48**(5): 2049-2052.

Sasakura, Y., S. Hirata, et al. (2002). "Characterization of a direct oxygen sensor heme protein from Escherichia coli - Effects of the heme redox states and mutations at the heme-binding site on catalysis and structure." Journal of Biological Chemistry **277**(26): 23821-23827.

Schenkman, J. B. and I. Jansson (2003). "The many roles of cytochrome b(5)." Pharmacology & Therapeutics **97**(2): 139-152.

Semrau, J. D., A. A. DiSpirito, et al. (2010). "Methanotrophs and copper." FEMS Microbiology Reviews **34**(4): 496-531.

Severinghaus, J. W., P. Astrup, et al. (1998). "Blood gas analysis and critical care medicine." American Journal of Respiratory and Critical Care Medicine **157**(4): S114-S122.

Siedow, J. N., S. Power, et al. (1978). "Preparation and Characterization of Highly Purified, Enzymatically Active Complex-III from Bakers Yeast " Journal of Biological Chemistry **253**(7): 2392-2399.

Smythe, G. A. and W. S. Caughey (1970). "Structure and Reactions of Heme a of Cytochrome c Oxidase." Journal of the Chemical Society D-Chemical Communications(13): 809-&.

Sogabe, S. and K. Miki (1995). "Refined crystal-structure of ferrocytochrome-*c*(2) from *Rhodopseudomonas viridis* at 1.6 ångstrom resolution." Journal of Molecular Biology **252**(2): 235-247.

Stein, L. Y., S. Yoon, et al. (2010). "Genome Sequence of the Obligate Methanotroph *Methylosinus trichosporium* Strain OB3b." Journal of Bacteriology **192**(24): 6497-6498.

Strittmatter, C. F. and E. G. Ball (1954). "The Intracellular Distribution of Cytochrome Components and of Oxidative Enzyme Activity in Rat Liver." Journal of Cellular and Comparative Physiology **43**(1): 57-78.

Stroebel, D., Y. Choquet, et al. (2003). "An atypical haem in the cytochrome b(6)f complex." Nature **426**(6965): 413-418.

Swanson, R., B. L. Trus, et al. (1977). "Tuna Cytochrome c at 2.0 Å Resolution. 1. Ferricytochrome Structure Analysis." Journal of Biological Chemistry **252**(2): 759-775.

Takano, T., B. L. Trus, et al. (1977). "Tuna Cytochrome c at 2.0 Å Resolution. 2. Ferrocytochrome Structure Analysis." Journal of Biological Chemistry **252**(2): 776-785.

Taylor, C. P. S. (1977). "EPR of Low-Spin heme Complexes - Relation of t2g Hole Model to Directional Properties of g-tensor, and a New Method for Calculating Ligand Field parameters." Biochimica Et Biophysica Acta **491**(1): 137-149.

Theorell, H. and A. Åkesson (1941). "Studies on cytochrome *c*. II. The optical properties of pure cytochrome *c* and some of its derivatives." Journal of the American Chemical Society **63**: 1812-1818.

Timkovich, R., D. Bergmann, et al. (1998). "Primary Sequence and Solution Conformation of Ferrocytochrome *c*-552 from *Nitrosomonas europaea*." Biophysical Journal **75**(4): 1964-1972.

Timkovich, R., M. S. Cork, et al. (1985). "Proposed Structure of Heme d, a Prosthetic Group of Bacterial Terminal Oxidases " Journal of the American Chemical Society **107**(21): 6069-6075.

Trautwein, A. X., E. Bill, et al. (1991). "Iron Containing Proteins and Related Analogs - Complementary Mössbauer, EPR and Magnetic Susceptibility Studies." Structure and Bonding **78**: 1-95.

Tsukihara, T., K. Shimokata, et al. (2003). "The low-spin heme of cytochrome c oxidase as the driving element of the proton-pumping process." Proceedings of the National Academy of Sciences of the United States of America **100**(26): 15304-15309.

Valenzuela, J. G., F. A. Walker, et al. (1995). "A Salivary Nitrophorin (Nitric Oxide Carrying Hemoprotein) in the Bedbug Cimex Lectuarius." Journal of Experimental Biology **198**(7): 1519-1526.

Valko, M., H. Morris, et al. (2005). "Metals, toxicity and oxidative stress." Current Medicinal Chemistry **12**(10): 1161-1208.

Virbasius, J. V. and R. C. Scarpulla (1988). "Structure and Expression of Rodent Genes Encoding the Testis Spesific Cytochrome c - Differences in Gene Structure and Evolution Between Somatic and Testicular Variants." Journal of Biological Chemistry **263**(14): 6791-6796.

Waldron, K. J., J. C. Rutherford, et al. (2009). "Metalloproteins and metal sensing." Nature **460**(7257): 823-830.

Walker, C. J. and R. D. Willows (1997). "Mechanism and regulation of Mg-chelatase." Biochemical Journal **327**: 321-333.

Walker, F. A. (1999). "Magnetic spectroscopic (EPR, ESEEM, Mossbauer, MCD and NMR) studies of low-spin ferriheme centers and their corresponding heme proteins." Coordination Chemistry Reviews **186**: 471-534.

Walker, F. A. (2004). "Models of the bis-histidine-ligated electron-transferring cytochromes. Comparative geometric and electronic structure of low-spin ferro- and ferrihemes." Chemical Reviews **104**(2): 589-615.

Walker, F. A. (2005). "Nitric oxide interaction with insect nitrophorins and thoughts on the electron configuration of the {FeNO}(6) complex." Journal of Inorganic Biochemistry **99**(1): 216-236.

Walker, F. A., B. H. Huynh, et al. (1986). "Models of the Cytochromes b - Effect of Axial Ligand Plane Orientation on the EPR and Mössbauer Spectra of Low-Spin Ferrihemes." Journal of the American Chemical Society **108**(17): 5288-5297.

Warburg, O. and H. S. Gewitz (1951). "*Cytohamin aus Herzmuskel " Hoppe-Seylers Zeitschrift Fur Physiologische Chemie **288**: 1-10.

Weber, P. C., F. R. Salemme, et al. (1981). "On the Evolutionary Relationship of the 4-alpha-helical Heme-proteins - The Comparison of Cytochrome b562 and Cytochrome c' " Journal of Biological Chemistry **256**(15): 7702-7704.

Weeratunga, S. K., S. Lovell, et al. (2010). "Structural Studies of Bacterioferritin B from Pseudomonas aeruginosa Suggest a Gating Mechanism for Iron Uptake via the Ferroxidase Center." Biochemistry **49**(6): 1160-1175.

Weichsel, A., J. F. Andersen, et al. (1998). "Crystal structures of a nitric oxide transport protein from a blood-sucking insect." Nature Structural Biology **5**(4): 304-309.

Wen, X. and K. L. Bren (2005). "Heme axial methionine fluxion in Pseudomonas aeruginosa Asn64Gln cytochrome c(551)." Inorganic Chemistry **44**(23): 8587-8593.

Wen, X. and K. L. Bren (2005). "Suppression of axial methionine fluxion in hydrogenobacter thermophilus Gln64Asn cytochrome c(552)." Biochemistry **44**(13): 5225-5233.

Wikstrom, M. K. F. (1977). "Proton Pump Coupled to Cytochrome *c* Oxidase in Mitochondria." Nature **266**(5599): 271-273.

Wilson, D. F., Erecinsk.M, et al. (1974). "Thermodynamic Relationships in Mitochondrial Oxidative Phosphorylation." Annual Review of Biophysics and Bioengineering **3**: 203-230.

Wilson, M. T. G., C. (1996). The Alkaline Transition in Ferricytochrome c. Cytochromes c - A Multidisciplinary Approach. R. I. M. Scott, A.G. Sausalito, University Science Books**:** 611 - 634.

Windsor, J. S. and G. W. Rodway (2007). "Heights and haematology: the story of haemoglobin at altitude." Postgraduate Medical Journal **83**(977): 148-151.

Wollaston, W. H. (1802). "On the Oblique Refraction of Iceland Crystal." Philosophical Transactions of the Royal Society of London **92**: 381 - 386.

Wood, P. M. (1983). "Why do *c*-type cytochromes exist?" FEBS Letters **164**(2): 223-226.

Wood, P. M. (1991). "Why do *c*-type cytochromes exist? - Reprise." Biochimica Et Biophysica Acta **1058**(1): 5-7.

Xia, D., C. A. Yu, et al. (1997). "Crystal structure of the cytochrome bc(1) complex from bovine heart mitochondria." Science **277**(5322): 60-66.

Yang, F., M. Knipp, et al. (2009). "H-1 and C-13 NMR spectroscopic studies of the ferriheme resonances of three low-spin complexes of wild-type nitrophorin 2 and

nitrophorin 2(V24E) as a function of pH." Journal of Biological Inorganic Chemistry **14**(7): 1077-1095.

Yasmin, S., S. C. Andrews, et al. (2011). "A New Role for Heme, Facilitating Release of Iron from the Bacterioferritin Iron Biomineral." Journal of Biological Chemistry **286**(5): 3473-3483.

Yatsunyk, L. A., M. D. Carducci, et al. (2003). "Low-spin ferriheme models of the cytochromes: Correlation of molecular structure with EPR spectral type." Journal of the American Chemical Society **125**(51): 15986-16005.

Yatsunyk, L. A., A. Dawson, et al. (2006). "Models of the cytochromes: Crystal structures and EPR spectral characterization of low-spin bis-imidazole complexes of (OETPP)Fe-III having intermediate ligand plane dihedral angles." Inorganic Chemistry **45**(14): 5417-5428.

Zavoisky, E. (1944). "The paramagnetic absorption of a solution in parallel fields." Journal of Physics-USSR **8**(1-6): 377-380.

Zavoisky, E. (1946). "Paramagnetic Absorption in Some Salts in Perpendicular Magnetic Fields." Zhurnal Eksperimentalnoi I Teoreticheskoi Fiziki **16**(7): 603-606.

Zhong, L. H., X. Wen, et al. (2004). "Heme axial methionine fluxionality in Hydrogenobacter thermophilus cytochrome C-552." Proceedings of the National Academy of Sciences of the United States of America **101**(23): 8637-8642.

Zhuang, J. Y., A. R. Reddi, et al. (2006). "Evaluating the roles of the heme a side chains in cytochrome c oxidase using designed heme proteins." Biochemistry **45**(41): 12530-12538.

Zoppellaro, G., K. L. Bren, et al. (2009). "Studies of Ferric Heme Proteins with Highly Anisotropic/Highly Axial Low Spin (S=1/2) Electron Paramagnetic Resonance Signals with bis-Histidine and Histidine-Methionine Axial Iron Coordination." Biopolymers **91**(12): 1064-1082.

Zoppellaro, G., E. Harbitz, et al. (2008). "Modulation of the Ligand-Field Anisotropy in a Series of Ferric Low-Spin Cytochrome c Mutants derived from *Pseudomonas aeruginosa* Cytochrome *c*-551 and *Nitrosomonas europaea* Cytochrome *c*-552: A Nuclear Magnetic Resonance and Electron Paramagnetic Resonance Study." Journal of the American Chemical Society **130**(46): 15348-15360.

Zoppellaro, G., T. Teschner, et al. (2006). "Low-temperature EPR and Mossbauer spectroscopy of two cytochromes with His-Met axial coordination exhibiting HALS signals." CHEMPHYSCHEM **7**(6): 1258-1267.

I

OPEN ACCESS Freely available online

PLoS one

Cytochrome c-554 from *Methylosinus trichosporium* OB3b; a Protein That Belongs to the Cytochrome c2 Family and Exhibits a HALS-Type EPR Signal

Espen Harbitz, K. Kristoffer Andersson*

Department of Molecular Biosciences, University of Oslo, Oslo, Norway

Abstract

A small soluble cytochrome *c*-554 purified from *Methylosinus trichosporium* OB3b has been purified and analyzed by amino acid sequencing, mass spectrometry, visible, CD and EPR spectroscopies. It is found to be a mono heme protein with a characteristic cytochrome *c* fold, thus fitting into the class of cytochrome c_2, which is the bacterial homologue of mitochondrial cytochrome *c*. The heme iron has a Histidine/Methionine axial ligation and exhibits a highly anisotropic/axial low spin (HALS) EPR signal, with a g_{max} at 3.40, and ligand field parameters $V/\xi = 0.99$, $\Delta/\xi = 4.57$. This gives the rhombicity $V/\Delta = 0.22$. The structural basis for this HALS EPR signal in Histidine/Methionine ligated hemes is not resolved. The ligand field parameters observed for cytochrome *c*-554 fits the observed pattern for other cytochromes with similar ligation and EPR behaviour.

Citation: Harbitz E, Andersson KK (2011) Cytochrome c-554 from *Methylosinus trichosporium* OB3b; a Protein That Belongs to the Cytochrome c2 Family and Exhibits a HALS-Type EPR Signal. PLoS ONE 6(7): e22014. doi:10.1371/journal.pone.0022014

Editor: Andreas Hofmann, Griffith University, Australia

Received May 9, 2011; **Accepted** June 10, 2011; **Published** July 18, 2011

Funding: This research was funded by the Norwegian Research Council (grant number 157855 [to EH] and grant number 177661/V30 [to KKA]). The funder had no role in study design, data collection and analysis, decision to publish, or preparation of the manuscript.

Competing Interests: The authors have declared that no competing interests exist.

* E-mail: k.k.andersson@imbv.uio.no

Introduction

The bacterium *Methylosinus trichosporium* OB3b is an obligatory methanotrophic gram-negative bacterium that can utilize methane as its only source of carbon and energy [1,2], and is one of the most studied methanotrophic alphaproteobacteria. In addition to be able to oxidize methane, *Methylosinus trichosporium* Ob3b is able to oxidize a broad spectrum of toxic and organic compounds otherwise difficult to degrade, including halogenated hydrocarbons as trichloroethylene [3,4]. This ability to oxidize potential biocides has led to an interest in using *Methylosinus trichosporium* OB3b for bioremediation of recalcitrant organic pollutants. *Methylosinus trichosporium* OB3b have two different enzyme systems capable of oxidizing methane, the soluble methane monooxygenase (sMMO) [5] and the membrane-bound particulate methane monooxygenase (pMMO) [6]. The expression of these enzyme systems (relative to each other) varies with the growth conditions, most importantly the copper concentration. High concentrations of copper(II) results in a high proportion of pMMO, while sMMO dominates at low copper(II) concentrations [2,5,6,7]. In bacterial methane metabolism, a soluble *c*-type cytochrome is known to be involved in the oxidation of methanol to methanal by methanol dehydrogenase in the periplasmic space [2,8].

C-type cytochromes are a diverse group of electron transfer proteins found in all areas of life. They are known to play important parts in key metabolic processes as respiration and photosynthesis. The covalent attachment of the heme group to the protein backbone is the key characteristic of these proteins and it is suggested that this is important for retaining the heme group outside the cytoplasm or in the mitochondrial intermembrane space [9], but it is proposed that heme attachment influences both heme reduction potential and ligand-iron interaction [10]. This attachment is formed by two (in some cases only one) thioether bonds with cysteine residues. The heme binding motif, Cys-X-X-Cys-His, is highly conserved and provides cysteine residues for the covalent attachment as well as a histidine axial ligand coordinating to the heme iron. The histidine is structurally constrained and the imidazole plane aligned roughly along the heme α-γ meso axis. The other ligand is most commonly methionine (e.g. mitochondrial cytochrome *c* [11], in the photosynthetic reaction centre [12] and soluble bacterial cytochromes [13,14,15]), but it can be histidine (e.g. cytochrome cd_1), the N-terminal amino group (cytochrome *f*) [16] or the iron can be five coordinated, as in cytochrome *c*' [17]. Historically different naming systems have been employed for the *c*-type cytochromes according to their physical properties, such as spectral features, redox potential or isoelectric point. In 1982, Ambler identified four major classes of *c*-type cytochromes based mainly on their sequence [18]. More recently Bertini and co-workers have added groups to this list when they scanned 188 genomes for cytochrome *c* domains, in order to obtain a wide coverage of the possible roles of *c*-type cytochromes [19]. The analysis of bacterial genomes revealed an astonishing variety in the number and types of *c*-type cytochromes encoded by different bacteria.

In this study we report purification and properties of a cytochrome *c*-554 from *Methylosinus trichosporium* OB3b, grown under pMMO expressing conditions. We compare this cytochrome with cytochrome *c*-555 from *Methylococcus capsulatus* (Bath), which was purified using the same protocol. We observe that these two cytochromes, both from methane oxidising bacteria, exhibit

markedly different ferric low-spin EPR spectra. Cytochrome *c*-554 from *Methylosinus trichosporium* OB3b exhibits a highly anisotropic/axial low spin (HALS) EPR signal, whereas cytochrome *c*-555 from *Methylococcus capsulatus* (Bath) exhibits a rhombic EPR signal. Since the relationship between structure and these EPR signals in His/Met-ligated hemes is not understood, the characterization of more His/Met coordinated heme systems may be helpful in explaining the physical basis of the different EPR spectral types [20].

Methods

Materials

Horse heart cytochrome *c* was obtained from Sigma-Aldrich, cytochrome *c*-552 from *Nitrosomonas europaea* was donated by Professor Alan B. Hooper, University of Minnesota [15,21], and cytochrome *c*-553 from *Bacillus pasteurii* was donated by Professor Stefano Ciurli, University of Bologna [13].

Bacterial Growth

Methylosinus trichosporium OB3b culture was obtained from the laboratory of John D. Lipscomb (University of Minnesota). Fermentation was conducted in a 10 L Biostat bioreactor (B. Braun, Melsungen) using a previously described culture medium [22] containing 10 μM copper sulphate. Cells were grown at 30°C and an agitation rate of 200–300 rpm and were purged with a 1:4 methane/air mixture. The pH in the fermentor was maintained at 6.8–7.0 by addition of 1 M H_2SO_4 (aq). Cells were harvested at an OD_{540} between 3.0 and 5.0. The bacterial culture was first cooled to 0°C using crushed ice. The cooled cell culture was filtered through a Millipore Masterflex Cross-flow filtration unit (45 μm) until the volume was 1 litre. Harvested cells were centrifuged at 7000 g for 10 minutes, washed in 50 mM Pipes buffer, pH 7.0, frozen in liquid nitrogen and stored at −80°C.

Protein purification of cytochrome *c*-554 from *Methylosinus trichosporium* OB3b

While still in the frozen state, 30 g cells were packed into the cooled **X-press**® (AB **BIOX**, Gothenburg) pressure cell [23]. Cells were disrupted by several passages through the 1 mm diameter orifice at a pressure of ~500 bars. This breaks the ice crystals irrespective of the cell membranes, thus disrupting the cells. The pressate was thawed and diluted with 120 ml 10 mM Tris HCl buffer, pH 8.2. The suspension was incubated with DNase I solution (80 Kunitz units) for 60 minutes at 4°C, and homogenized and centrifuged at 12.000 g for 20 minutes and then at 75.000 g for 3 hours. Ammonium sulphate was dissolved in the supernatant until the solution was 75% saturated, stirred for 60 minutes at 4°C, and centrifuged at 13.000 g for 30 minutes. The supernatant was applied to a phenyl sepharose column (1.5 cm ×30 cm), equilibrated with 1.5 M $(NH_4)_2SO_4$ in 10 mM Tris HCl buffer (pH 8.2). The protein was eluted with a linear gradient from 1.5 M to 0 M $(NH_4)_2SO_4$. The eluted fractions with significant absorption at 410 nm were collected and concentrated in an Amicon® ultrafiltration cell (10 kDa filter cut-off). The ionic strength of the sample was decreased using a NAP- 10 column (GE Healthcare), which is a standardized Sephadex G-25 gel filtration column, before it was applied to a CM sepharose column (1.5 cm×20 cm), which had been equilibrated with 10 mM Tris HCl buffer (pH 8.2). The protein was eluted with a linear gradient from 0 to 0.15 M KCl in 10 mM Tris HCl buffer (pH 8.2), and then concentrated. The protein solution was applied to a Sephadex G-75 gel filtration column (1.5 cm×30 cm) equilibrated with 10 mM Tris HCl buffer (pH 8.2), concentrated and stored at −80°C. The same procedure was used to purify cytochrome *c*-555 from *Methylococcus capsulatus* (Bath).

Protein Sequencing

Protein sequencing was performed by automatic Edman degradation on an Applied Biosystems 477A Protein Sequencer (Applied Biosystems, Foster City, CA, USA) with an online 120A PTH amino acid analyser in the lab of Knut Sletten [24]. Cyanogen bromide (CNBr) cleavage of the protein was performed by dissolving 50 nmol freeze dried protein in 70% formic acid followed by an addition of a 50-fold excess of CNBr [25]. The mixture was left to incubate in darkness at 20°C for 24 hours. The CNBr was removed by evaporation before sequencing. The peptide sequences obtained was compared with the newly released genome [26] using TBLASTN, which searches a translated nucleotide sequence using a protein query [27]. The full peptide sequence identified was modelled on the structure peptide backbone of ferrocytochrome c_2 from *Rhodopseudomonas viridis* (1CO6.pdb) using SWISS-MODEL [28]. The protein sequence data reported in this paper will appear in the UniProt Knowledgebase under the accession number D5QVH0.

EPR Spectroscopy

The EPR spectra were acquired with a Bruker Elexsys 300E 10/12 X–band spectrometer equipped with a Bruker ER4116DM dual mode resonator cavity. A HeFlow cryostat (ESR 900, Oxford Instruments) allowed temperature regulation of the sample in the region 3.6 K to 100 K. The EPR samples were prepared by employing fast freezing procedures (from 273 K to77 K) of the protein solutions placed in EPR tubes. In all the measurements for cytochromes *c*, the EPR signals were too broad to detect above 30 K; thus most of the EPR spectra were collected at 10 K. The experimental conditions was: 9.65 GHz, modulation amplitude 1 mT, modulation frequency 100 kHz, sweep time168 s, time constant 82 ms, 4×10^4 gain, and the spectra was recorded in perpendicular mode. The spectra were recorded at 10±0.5 K, except for the temperature behaviour studies were data were recorded at 7, 13, 16, 21, 26, 31 and 36 K. The EPR spectra was recorded under non-saturating microwave power, with the exception of the microwave power saturation studies performed at 0.08, 0.2, 0.4, 0.8, 2.01, 6.35, 15.9, 63.5 and 159 mW. The spectral features was simulated with WINEPR SimFonia version 1.25 provided by Bruker.

Light absorption spectroscopy

UV-Vis transitions were observed on a HP8452A Spectrophotometer and a Jasco J-810 Spectropolarimeter. The heme content was quantified using alkaline pyridine hemochrome [29], which gives distinct absorption band, where the extinction coefficients vary only with the type of heme. (For heme *c* the extinction coefficients for the α- and β-bands are $\varepsilon_{551} = 29.1\ mM^{-1}\ cm^{-1}$ and $\varepsilon_{522} = 18.6\ mM^{-1}\ cm^{-1}$ [29].) A few grains of dithionite were added to the purified cytochrome *c* solution (50 μM) before an equal amount of a stock solution containing 0.15 M NaOH and 2.1 M pyridine was mixed with the protein solution. The heme concentration measured using alkaline pyridine hemochrome [29], was used to calculate extinction coefficients for the initial cytochrome solution.

Mass spectroscopy and heme cleavage

The protein mass was established using a Voyager-RP DE mass spectrometer (Applied Biosystems, Foster City, CA, USA) in the linear positive ion mode. Acceleration voltage, grid voltage and the

delay time between ion production and extraction were adjusted to get optimal peak resolution for each sample. For each spectrum, 100 single scans were accumulated. The matrix, sinapinic acid (3,5-dimethoxy-4-hydroxy cinnamic acid (D-7927, Sigma-Aldrich, St. Louis, MI, USA)) was dissolved to saturation in a 1:1 (v/v) mixture of acetonitrile and 0,1% (v) aqueous trifluoroacetic acid. Equal volumes of sample and matrix solution were mixed on the sample plate and air dried. All data were calibrated using an external calibration standard mixture (Applied Biosystems, Foster City, CA, USA). The *c*-type hemes was cleaved from the protein by reacting with 2-nitrophenylsulfenylchloride (2-NPS-Cl). It was performed by mixing 80 µl cytochrome *c* solution (20–30 µM) in 50% acetic acid with 40 µl 2-NPS-Cl (4 mM in acetic acid) and incubated for 10 minutes. Removal of 2-NPS from modified cysteine residues were done by adding 80 µl 0.4% mercaptoethanol (in a 10 M Urea solution) and incubated for another 10 minutes before the protein was desalted on a NAP-5 column equilibrated with 10% acetic acid. In the fractions collected after desalting there were an absence of the characteristic heme absorption bands, but a peak at 365 nm was observed confirming the presence of tryptophan residues modified by 2-NPS-Cl [30]. Ferrous and ferric cytochrome were prepared by addition of an excess of sodium dithionite, $Na_2S_2O_4$, or potassium ferricyanide, $K_3Fe(CN)_6$, to the cytochrome solution, respectively, and excess reagents were removed on a NAP-5 column.

Results

Protein purification of cytochrome *c*-554

The purification procedure was monitored with light absorption by observing the ratio A_{410} /A_{280} as a measure of the heme to protein ratio. At the end of the purification procedure, this ratio approached 8. This is a reasonable value for a pure protein sample when compared with our measured extinction coefficient and the amino acids found in the protein sequence. SDS-PAGE revealed no protein impurities and suggested a molecular weight of about 13000 Da (data not shown). This is in good agreement with the mass obtained by mass spectrometry (see below).

Visible absorption and CD spectra indicates methionine ligation of cytochrome *c*-554

The absorption spectrum of the reduced form the cytochrome had α-, β- and Soret bands at 554, 524 and 416 nm, respectively. Upon oxidation, the Soret band shifted to 410 nm and the β-band to 526 nm (Figure 1A). Heme concentrations were calculated using pyridine hemochrome to obtain an accurate estimate of heme protein content [29]. These protein concentrations were used to calculate the extinction coefficients. The absorption spectrum of the reduced cytochrome has the following extinction coefficients: $\varepsilon_{416} = 126\ mM^{-1}\ cm^{-1}$, $\varepsilon_{524} = 17\ mM^{-1}\ cm^{-1}$ and $\varepsilon_{554} = 24\ mM^{-1}\ cm^{-1}$. The oxidized cytochrome has the extinction coefficients: $\varepsilon_{410} = 116\ mM^{-1}\ cm^{-1}$ and $\varepsilon_{526} = 14\ m M^{-1}\ cm^{-1}$. The oxidized protein also exhibited a weak band at 695 nm, which is indicative of methionine ligation [31]. The feature at 695 nm was further confirmed by CD spectroscopy [21]. The observed negative CD feature corresponding to this absorption band is red-shifted compared to mammalian cytochrome *c*, similar to what we observe in cytochrome *c*-552 from *Nitrosomonas europaea*, which has the same His/Met heme ligation and a known 3D structure [11,15] (Figure 1B).

Mass spectroscopy reveals a single heme group

There exist many classes of *c*-type cytochromes, with varying number of heme groups attached. Determining the number of hemes attached to a protein might prove difficult, as seen in the case of cytochrome *c*-554 from *Nitrosomonas europaea*, which were believed to contain two hemes but were later found to contain four

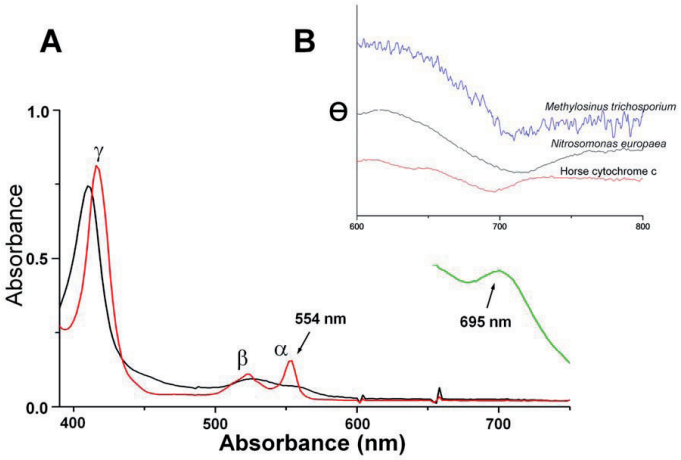

Figure 1. Absorption and CD spectra of cytochrome *c*-554 from *Methylosinus trichosporium* OB3b. A. Visible absorption spectra of a 7 µM solution of the reduced and oxidized cytochrome *c*-554 from *Methylosinus trichosporium* OB3b. The α-band in the reduced spectrum has a maximum at 554 nm used to name the cytochrome. The spectrum of a 83 µM solution of the oxidized protein exhibits a peak at 695 nm in the oxidised spectrum is indicative of methionine ligation to the heme. B. Circular dichroism of a 60 µM solution of cytochrome *c*-554 (magnified 10 times) is compared with a 790 µM solution of cytochrome *c*-552 from *Nitrosomonas europaea* and a 200 µM solution of cytochrome *c* from horse heart. The circular dichroism at the methionine peak shows that the cytochrome *c*-554 has stronger similarities with cytochrome *c*-552 from *Nitrosomonas europaea* than cytochrome *c* from horse heart.
doi:10.1371/journal.pone.0022014.g001

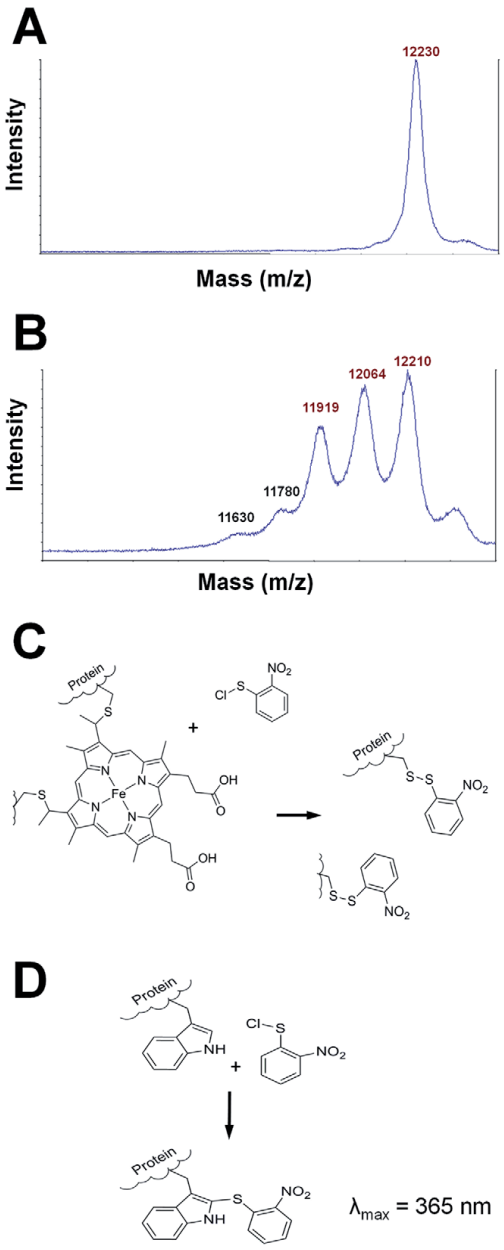

Figure 2. Mass determination and heme cleavage of cytochrome *c*-554 from *Methylosinus trichosporium* OB3b. A. Mass spectrum of the native cytochrome *c*-554 from Methylosinus trichosporium OB3b. B. Mass spectrum of cytochrome *c*-554 after treatment with 2-NPS. The number of peaks is due to protein adducts with different number of added 2-NPS molecules. C. The reaction of 2-NPS with the covalent heme attachment, resulting in a disulphide link between 2-NPS and the protein and loss of the heme group. D. 2-NPS reacts with tryptophan, creating a chromophore with an absorption maximum at 365 nm [30].
doi:10.1371/journal.pone.0022014.g002

hemes [32,33]. To establish the number of heme groups and to obtain an accurate mass determination, MALDI-TOF MS was performed. The molecular weight of the cytochrome was estimated to be 12230±15 Da (Figure 2A). Treatment with 2-nitrophenylsulfenylchloride (2-NPS-Cl) was used to cleave the heme group. The 2-NPS-Cl treated protein exhibited peaks corresponding to a loss of one heme group (Figure 2B). No peaks at lower mass to charge ratios were found, indicating the presence of a single heme group in the protein. Treatment with 2-NPSCl cleaves of the heme group by breaking the thioether bond between the heme group and the cysteine in the CXXCH heme binding motif (Figure 2C). 2-NPS will furthermore react with tryptophan residues to create a chromophore with an absorption maximum at 365 nm (Figure 2D). The observation of this chromophore was used to trace the protein after removal of the heme group, and furthermore suggested the presence of two tryptophan residues in the protein.

Amino acid sequence of cytochrome *c*-554 from *Methylosinus trichosporium* OB3b

Two parts of the cytochrome *c*-554 from *Methylosinus trichosporium* OB3b were sequenced using Edman degradation [34]. The first 39 amino acids on the N-terminal were determined to be AGDPAAGEKVFNKCKACHQVGETAKNAVAPELNGIDGRK. After cyanogenbromide (CNBr) treatment two peptide fragments were observed, which verified the presence of only one methionine residue in this sequence. The amino acid sequence obtained from the second peptide is MIFPGLSSENDQANVWAYLSQFGADGKK. Sequence alignment indicates that this is the C-terminal part of the protein, and that the methionine at the beginning of the second fragment is the sixth heme axial ligand. The middle part of the protein has not been sequenced. The two sequences, bridged by a gap of unknown length, were aligned using tBlastn with the complete genome of *Methylosinus trichosporium* OB3b [26,27]. Full identity was found with the bases 13660–13980 in contig00046 of the genome. The complete sequence of the protein contains the following 108 amino acids: H_2N-AGDPAAGEKVFNKCKACHQVGETAKNAVAPELNGIDGRKSASAEGYNYSEPFKALGITWDEAQFKEFIKNPKAKVPGTKMIFPGLSSENDQANVWAYLSQFGADGKKK-COOH. The heme binding motif and the iron coordinating methionine residue is underlined. The complete protein sequence contains only one heme binding motif and two tryptophans in agreement with the observations from mass spectrometry. There is only one methionine residue in the protein, in position 80, in good agreement with the cyanogenbromide cleavage. The genomic sequence revealed a 24 amino acid signal sequence, MKSISMLTLAASVAFAVTAGQAVA, confirming the periplasmic location of this protein [35]. Based on the primary sequence, a theoretical pI value of 8.55 was calculated using the program ProtParam on the ExPASy server [9,36].

The sequence was aligned with protein and nucleotide sequence databases using protein blast and tBlastn [27]. The best alignment is found with a *c*-type cytochrome from the genome sequence of *Nitrobacter winogradskyi* strain Nb-255, which has 64% identical residues and 78% positive residues (identical residues or conservative mutations). All best alignments represent *c*-type cytochromes from bacteria belonging to the alphaproteobacteria in the order *Rhizobiales*, in which *Methylosinus trichosporium* OB3b is included. The most similar alignment with a protein with known

3D structure is ferrocytochrome c_2 from *Rhodopseudomonas viridis* with 56 (52%) identical residues, a total of 74 (69%) positive residues and no gaps (pdb-id: 1CO6) [37]. Homology modelling of the tertiary structure using this cytochrome as template reveals a tertiary structure similar to the cytochrome *c* fold of mitochondrial cytochrome *c* (Figure 3) [11,38]. The identity with horse heart cytochrome *c* is 30.5% (33 out of 108 residues).

EPR spectroscopy shows that cytochrome *c*-554 exhibits a highly anisotropic low spin (HALS) signal

Electron paramagnetic resonance (EPR) spectroscopy probes unpaired electron in a sample. As the only unpaired electrons in proteins occur at metal ions or in free radical enzyme mechanisms, EPR is an excellent tool to study the chemically active part of a protein without interference from the protein backbone. Cytochrome *c*-554 from *Methylosinus trichosporium* OB3b exhibits a ferric HALS (Highly Axial Low-Spin or Highly Anisotropic Low-Spin ($S = ½$)) also called Type I EPR signal by the nomenclature introduced by F. Ann Walker [39] when subjected to low temperature EPR spectroscopy, with a g_{max} value of 3.40 (Figure 4C). HALS EPR signals are also known as "large g_{max}" signals. This kind of signals have been observed in cytochromes with His/His, His/amine and His/Met coordination of the heme iron, and the main characteristic of these signals is a *g*-value higher than 3.3 [20,39,40,41]. Because of the nature of the very broad HALS EPR signal, direct assignment of all three *g*-values is generally not possible. The microwave absorption amplitude decays slowly and extends to high magnetic fields, which results in

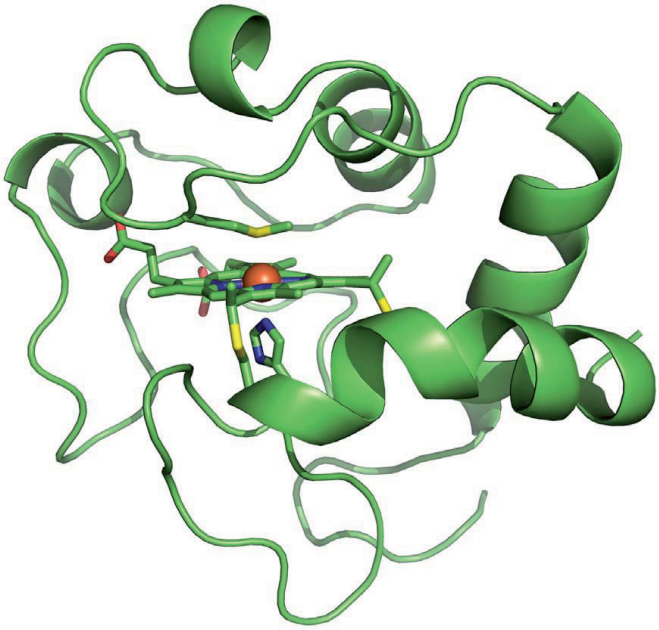

```
M. trichosporium   AGDPAAGEKVFN-KCKACHQVGETAKNAVAPELNGIDGRK 39
R. viridis         -QDAASGEQVFK-QCLVCHSIGPGAKNKVGPVLNGLFGRH 38
Horse heart        XGDVEKGKKIFVQKCAQCHTVEKGGKHKTGPNLHGLFGRK 40
                     *   *:::*  :*  ** :   .*: ..* *:*: **:

M. trichosporium   SASAEGYNYSEPFKALGITWDEAQFKEFIKNPKAKVPGTK 79
R. Viridis         SGTIEGFAYSDANKNSGITWTEEVFREYIRDPKAKIPGTK 78
Horse heart        TGQAPGFTYTDANKNKGITWKEETLMEYLENPKKYIPGTK 80
                   :.   *: *:::. *  **** *  : *:::.:**  :****

M. trichosporium   MIFPGLSSENDQANVWAYLSQFGADGKKK 108
R. viridis         MIFAGVKDEQKVSDLIAYIKQFNADGSKK 107
Horse heart        MIFAGIKKKTEREDLIAYLKKATNE---- 105
                   ***.*:..: .  :: **:.:   :
```

Figure 3. Homology model of cytochrome *c*-554 from *Methylosinus trichosporium* OB3b. The structure template used is cytochrome c_2 from *Rhodopseudomonas viridis* (PDBid: 1CO6) [37]. The amino acid sequence of these two proteins has 56 (52%) identical residues and a total of 74 (69%) positives (identical residues or conservative mutations). High similarity with the mitochondrial cytochrome *c* is found, and sequence alignment reveals a highly conserved region in the loop containing the heme axial ligand methionine. The molecular drawing was made with Pymol, DeLano Scientific, San Carlos, CA.
doi:10.1371/journal.pone.0022014.g003

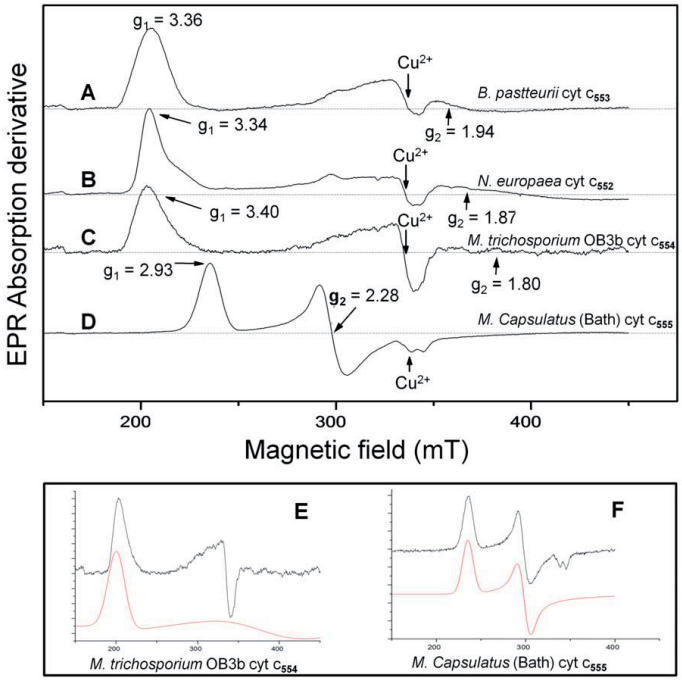

Figure 4. EPR spectroscopy of c-type cytochromes. X-band EPR spectra of cytochromes *c* from: A. *Bacillus pasteurii* (cytochrome *c*-553) [44], B. *Nitrosomonas europaea* (cytochrome *c*-552) [44], C. *Methylosinus trichosporium* OB3b (cytochrome *c*-554), and D. *Methylococcus capsulatus* (Bath) (cytochrome *c*-555). The protein solutions were prepared in 50 mM HEPES buffer at pH 7.5, and the spectra were recorded in perpendicular mode at 10 K with 2 mW microwave power, modulation amplitude 1 mT, modulation frequency 100 kHz, sweep time 168 s, time constant 82 ms and 4×10^4 gain. E. Simulation of the HALS EPR spectrum C (red). F. Simulation of the rhombic EPR spectrum D (red).
doi:10.1371/journal.pone.0022014.g004

a weak slope, and hence small amplitudes in the 1st derivative spectrum. Usually low-spin ferric hemes exhibit rhombic EPR spectra where two distinct *g*-values can be clearly resolved (Figure 4D). In the HALS EPR spectra, the last two *g*-values are very poorly resolved. HALS EPR spectra can be observed in cytochromes *c* from markedly different bacterial species like *Bacillus pasteurii*, *Nitrosomonas europaea* and *Methylosinus trichosporium* OB3b (Figure 4A, B and C), while other bacterial cytochromes *c* like cytochrome *c*-555 from *Methylococcus capsulatus* (Bath) (see below) exhibit rhombic EPR spectra with *g*-values at 2.93, 2.28 and 1.49 (Figure 4D and Table 1).

Table 1. Ligand field and g-tensor values for the EPR signal from the *c*-type cytochromes (EPR spectra shown in Figure 4).

	g_{max}	g_{mid}	g_{min}	V/ξ	Δ/ξ	V/Δ	Ref
B. pasteurii c-553	3.36	1.94	0.98	1.00	3.18	0.31	[44]
N. europaea c-552	3.34	1.87	1.17	1.09	4.45	0.24	[44]
M. trichosporium OB3b *c*-554	3.4	1.8	1.1	0.99	4.57	0.22	This work
M. capsulatus (Bath) *c*-555	2.93	2.28	1.49	1.87	3.06	0.61	This work

doi:10.1371/journal.pone.0022014.t001

The line width of the two lower *g*-components (at higher magnetic field) in the HALS EPR signals is very broad and can not be accurately assigned from the spectrum. Simulations of the EPR signal shows that the spectrum is best fit with $g_y = 1.8$ (Figure 4E). The g_x-value was too broad for any meaningful simulation, and was calculated to be 1.1 using the equation $g_z^2 + g_y^2 + g_x^2 = 16$ [40]. Using the equations of Taylor the crystal field parameters were calculated to be $V/\xi = 0.994$, $\Delta/\xi = 4.57$. This gives the rhombicity $V/\Delta = 0.22$ and $a^2 + b^2 + c^2 = 1.0006$, which is in the acceptable range demanded by this analysis [41]. These are refined values compared to what we previously reported [42], still fitting the observed trend for the *c*-type cytochromes with His/Met ligation that exhibit a ferric HALS EPR signal.

At 10 K this EPR signal is difficult to saturate, revealed by a relatively high microwave power saturation value ($P_{½}$). The $P_{½}$ value was determined for the HALS EPR signal from cytochrome *c*-554 from *Methylosinus trichosporium* OB3b using the equation [43]:

$$\frac{S}{\sqrt{P}} = \frac{K}{\left(1+\left(\frac{P}{P_{1/2}}\right)\right)^{\frac{b}{2}}}$$

Where **S** denotes the double integral of the EPR signal, **K** is a normalisation factor, **P** is the microwave power, ***b*** is a component relating to the type of relaxation and $\mathbf{P}_{½}$ is the microwave power

at half saturation. The b factor can vary between 1 for a completely inhomogeneous relaxation, and 3 for a completely homogenous relaxation. The microwave power saturation behaviour of *Methylosinus trichosporium* OB3b cytochrome *c*-554 was simulated with a *b* factor of 1 and indicates a $P_{½}$ value of 44 mW±9 mW (Figure 5C). All the studied *c*-type cytochromes that exhibit HALS EPR spectra show $P_{½}$ values above 40 mW at 10 K [44,45], indicating that high saturation midpoint may be a general feature of the HALS EPR signal.

EPR spectra of the "*g*-max" signal were recorded at seven different temperatures ranging from 7 K to 36 K under non-saturating conditions (microwave power 0.8 mW) with all other instrumental parameters kept constant (Figure 5A). At 36 K, the EPR signal was barely visible. This is similar to the temperature behaviour of the other HALS EPR signals studied, and consistent with the former notion that these signals are not readily observed above 20 K [39,44]. Figure 5B shows how the double integral of the EPR signal varies with the inverse absolute temperature. The linear behaviour shows that the magnetisation follows the Curie law in this temperature interval. This implies that the unpaired electron in the ferric cytochrome behaves like an ideal spin-½ paramagnet in the temperature range 7 K to 36 K, hence it is not influenced by neighbouring paramagnetic species.

Cytochrome *c*-555 from *Methylococcus capsulatus* (Bath)

Frozen cells of the methane oxidizing gammaproteobacterium *Methylococcus capsulatus* (Bath) was received as a generous gift from DB Lab A/S in Odense, Denmark [46]. The same purification protocol as was used for cytochrome *c*-554 from *Methylosinus trichosporium* OB3b was used to purify a *c*-type protein from this bacterium. This *c*-type cytochrome has a molecular weight of 11120 Da as determined by MALDI-TOF MS. The first 14 amino acids were sequenced using Edman degradation and showed full identity with the cytochrome *c*-555 previously reported by Ambler et al. [47]. This cytochrome exhibits a rhombic EPR signal (Figure 4D, 4F and Table 1) where the crystal field parameters were calculated to be $V/\xi = 1.87$ and $\Delta/\xi = 3.06$. This gives the rhombicity $V/\Delta = 0.61$ and $a^2 + b^2 + c^2 = 1.003$.

Discussion

HALS EPR signals can occur both in Histidine/Methionine ligated hemes like in cytochromes c_2, and in bis-Histidine ligated hemes. In bis-Histidine ligated hemes, a relation between the geometry of the histidines and the different EPR spectra has been found [39,48]. A similar structural basis for this signal in His/Met coordinated hemes is not understood [20,21,40,42,44,45,49]. The derived ligand field parameters for cytochrome *c*-554 from *Methylosinus trichosporium* Ob3b is $V/\xi = 0.99$ and $\Delta/\xi = 4.57$, and a rhombicity $V/\Delta = 0.22$. This is similar to what we find in other *c*-type cytochromes (Table 1) where we observe that proteins exhibiting HALS EPR signals have V/ξ around 1.0 and a rhombicity lower than 1/3.

Six coordinated *c*-type cytochromes are electron transfer proteins, but the biological role of cytochrome *c*-554 from *Methylosinus trichosporium* Ob3b has not been elucidated. The homologues of cytochrome *c*-554 in the group cytochrome c_2 is known to mediate electron transfer between bc_1 complexes and cytochrome *c* oxidases during aerobic growth [19]. A similar role is possible for this cytochrome, as the high theoretical pI suggests a weak membrane association and the signal sequence suggests a periplasmic localisation, which is a common localisation for cytochromes *c* [50], or it might be involved in the metabolism of methane. The genome of *Methylosinus trichosporium* OB3b contains

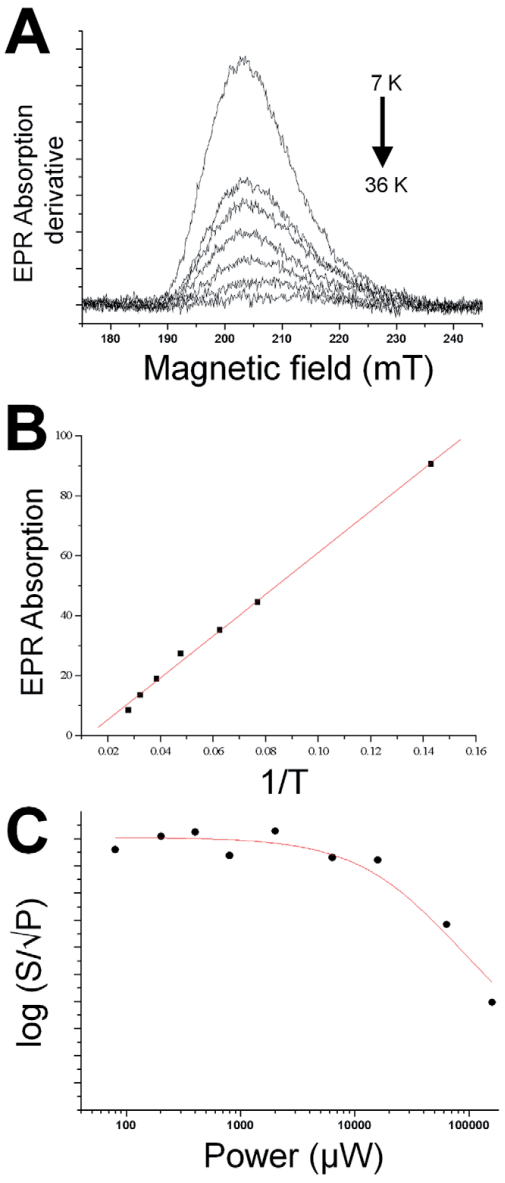

Figure 5. Temperature and microwave-power behaviour of the EPR signal of cytochrome *c*-554 from *Methylosinus trichosporium* OB3b. A. Temperature dependence of the HALS EPR spectrum. The spectra were recorded at 800 μW and the temperatures were 7, 13, 16, 21, 26, 31 and 36 respectively. B. The double integral of g-max plotted against the inverse temperature (1/T). The line represents the linear fit according to the Curie-law. C. Power saturation of the EPR spectrum. S equals the double integral of g-max, and P is the microwave power. The line is a simulated power saturation behaviour assuming a b-value of 1, indicating a $P_{½}$ value of 44 mW. The spectra were recorded in perpendicular mode with modulation amplitude 1 mT, modulation frequency 100 kHz, sweep time 168 s, time constant 82 ms and 4×10^4 gain.
doi:10.1371/journal.pone.0022014.g005

several (around 10) putative *c*-type cytochromes, but only a few is mentioned in the literature [51]. The homology with mitochondrial cytochrome *c* is not unreasonable as the mitochondrion is believed to originate from another alphaproteobacterium [52].

Cytochrome *c*-554 belongs to the class of cytochrome c_2. The homologous mitochondrial cytochrome *c* has a rhombic EPR spectrum with *g*-values of 3.06, 2.24 and 1.24 [53] and the related membrane interacting cytochrome c_2 from *Rhodobacter sphaeroides* has *g*-values of 3.29, 2.06 and 1.14 at neutral pH [54]. Both of these have known crystal structure [55]. Interestingly, the axial methionine ligand in the latter structure can be lost, as also suggested for horse heart cytochrome *c* at high pH [56]. This indicates, together with the fluxionality of the methionine ligand in *Nitrosomonas europaea* cytochrome *c*-552 that the methionine is loosely coordinated to the iron. The *g*-values of cytochrome *c*-554 from *Methylosinus trichosporium* OB3b is clearly HALS, and represent the high end of the g_{max} range observed for the small soluble cytochromes c [42]. The mitochondrial cytochrome *c* is found in low g_{max} end of this range, and cytochrome c_2 from *Rhodobacter sphaeroides* is in the middle of this range. The homology with these membrane interacting cytochromes further strengthens the idea that cytochrome *c*-554 is membrane associated, and might have a weakly coordinated axial methionine. This study further indicate that subtle differences in the His/ Met ligated heme proteins can modulate the low-spin EPR signal [42,45]. This is in agreement with preliminary, unpublished crystallographic studies, by Kara Bren's and K.Kristoffer Andersson's laboratories, on the *Nitrosomonas europaea* cytochrome *c*-552 mutant without the HALS EPR signal.

Acknowledgments

Thanks are due to Siv Fauchald who worked on this protein as her 'hovedfag' thesis, and Dr. Bettina Katterle who was responsible for the cultivation on *Methylosinus trichosporium* OB3b and knowledge transfer in the lab. We are also grateful to Hamid Shegarfi and Innocent O. Chukwu, who helped in growing the bacterium and assisted in the purification procedure, and Dr. Giorgio Zoppellaro who performed the EPR on *Methylococcus capsulatus (Bath)* cytochrome *c*-555, and assisted with the EPR analysis.

Author Contributions

Conceived and designed the experiments: KKA EH. Performed the experiments: EH KKA. Analyzed the data: EH KKA. Contributed reagents/materials/analysis tools: EH KKA. Wrote the paper: EH KKA.

References

1. Whittenbury R, Phillips KC, Wilkinson JF (1970) Enrichment, isolation and some properties of methane-utilizing bacteria. J Gen Microbiol 61: 205–218.
2. Semrau JD, DiSpirito AA, Yoon S (2010) Methanotrophs and copper. FEMS Microbiol Rev 34: 496–531.
3. Fox BG, Borneman JG, Wackett LP, Lipscomb JD (1990) Haloalkene Oxidation by the Soluble Methane Monooxygenase from *Methylosinus trichosporium* OB3b - Mechanistic and Environmental Implications. Biochemistry 29: 6419–6427.
4. Sullivan JP, Dickinson D, Chase HA (1998) Methanotrophs, *Methylosinus trichosporium* OB3b, sMMO, and their application to bioremediation. Crit Rev Microbiol 24: 335–373.
5. Lipscomb JD (1994) Biochemistry of the Soluble Methane Monooxygenase. Annu Rev Microbiol 48: 371–399.
6. Balasubramanian R, Rosenzweig AC (2007) Structural and mechanistic insights into methane oxidation by particulate methane monooxygenase. Acc Chem Res 40: 573–580.
7. Hakemian AS, Rosenzweig AC (2007) The biochemistry of methane oxidation. Annu Rev Biochem 76: 223–241.
8. Dales SL, Anthony C (1995) The Interaction of Methanol Dehydrogenase and its Cytochrome Electron Acceptor. Biochem J 312: 261–265.
9. Wood PM (1983) Why do *c*-type cytochromes exist? FEBS Lett 164: 223–226.
10. Bowman SEJ, Bren KL (2008) The chemistry and biochemistry of heme c: functional bases for covalent attachment. Nat Prod Rep 25: 1118–1130.
11. Bushnell GW, Louie GV, Brayer GD (1990) High-Resolution 3-Dimentional Structure of Horse Heart Cytochrome *c*. J Mol Biol 214: 585–595.
12. Lancaster CRD, Michel H (1996) Three-dimensional structures of photosynthetic reaction centers. Photosynth Res 48: 65–74.
13. Benini S, Gonzalez A, Rypniewski WR, Wilson KS, Van Beeumen JJ, et al. (2000) Crystal structure of oxidized *Bacillus pasteurii* cytochrome c(553) at 0.97-angstrom resolution. Biochemistry 39: 13115–13126.
14. Salemme FR, Freer ST, Xuong NH, Alden RA, Kraut J (1973) Structure of Oxidized Cytochrome c_2 of *Rhodospirillum rubrum*. J Biol Chem 248: 3910–3921.
15. Timkovich R, Bergmann D, Arciero DM, Hooper AB (1998) Primary Sequence and Solution Conformation of Ferrocytochrome c-552 from *Nitrosomonas europaea*. Biophys J 75: 1964–1972.
16. Carrell CJ, Schlarb BG, Bendall DS, Howe CJ, Cramer WA, et al. (1999) Structure of the soluble domain of cytochrome *f* from the cyanobacterium *Phormidium laminosum*. Biochemistry 38: 9590–9599.
17. Finzel BC, Weber PC, Hardman KD, Salemme FR (1985) Structure of Ferricytochrome c' from *Rhodospirillum Molischianum* at 1.67 Å resolution. J Mol Biol 186: 627–643.
18. Ambler RP (1982) The Structure an Classification of Cytochromes *c*. In: Kaplan NO, Robinson, A, eds. From Cyclotrons to Cytochromes. New York: Academic Press. pp 263–280.
19. Bertini I, Cavallaro G, Rosato A (2006) Cytochrome *c*: Occurrence and functions. Chem Rev 106: 90–115.
20. Salerno JC (1984) Cytochrome Electron Spin resonance Line Shapes, Ligand Field, and Components Stoichiometry in Ubiquinol Cytochrome *c* Oxidoreductase. J Biol Chem 259: 2331–2336.
21. Arciero DM, Peng QY, Peterson J, Hooper AB (1994) Identification of Axial Ligands of Cytochrome C(552) from *Nitrosomonas europaea*. FEBS Lett 342: 217–220.
22. Cornish A, Nicholls KM, Scott D, Hunter BK, Aston WJ, et al. (1984) *In vivo* C-13 NMR Investigations of methanol oxidation by the obligate methanotroph *Methylosinus trichosporium* OB3B. J Gen Microbiol 130: 2565–2575.
23. Magnusson KE, Edebo L (1976) Large-Scale Disintegration of Microorganisms by Freeze-Pressing. Biotechnol Bioeng 18: 975–986.
24. Kjaeraas S, Husby G, Sletten K (2006) The amino acid sequence of an AL-protein, AL-KH, isolated from the heart of a patient with Waldenstroms macroglobulinemia and amyloidosis. Amyloid 13: 260–262.
25. Gross E, Witkop B (1961) Selective cleavage of methionyl peptide bonds in ribonuclease with cyanogen bromide. J Am Chem Soc 83: 1510–1511.
26. Stein LY, Yoon S, Semrau JD, DiSpirito AA, Crombie A, et al. (2010) Genome Sequence of the Obligate Methanotroph *Methylosinus trichosporium* Strain OB3b. J Bacteriol 192: 6497–6498.
27. Altschul SF, Madden TL, Schaffer AA, Zhang JH, Zhang Z, et al. (1997) Gapped BLAST and PSI-BLAST: a new generation of protein database search programs. Nucleic Acids Res 25: 3389–3402.
28. Arnold K, Bordoli L, Kopp J, Schwede T (2006) The SWISS-MODEL workspace: a web-based environment for protein structure homology modelling. Bioinformatics 22: 195–201.
29. Falk JE (1964) Haems. I. Determination As Pyridine Haemochromes. In: Falk JE, ed. Porphyrins and Metalloporphyrins. Amsterdam: Elsevier Publishing. pp 181–188.
30. Fontana A, Veronese FM, Boccu E (1973) Reaction of sulfenyl halides with cytochrome - novel method for heme cleavage. FEBS Lett 32: 135–138.
31. Stellwagen E, Cass R (1974) Alkaline isomerization of ferricytochrome-c from *Euglena Gracilis*. Biochem Biophys Res Commun 60: 371–375.
32. Yamanaka T, Shinra M (1974) Cytochrome c-552 and cytochrome c-554 derived from *Nitrosomonas europaea* - purification, properties, and their function in hydroxylamine oxidation. J Biochem 75: 1265–1273.
33. Andersson KK, Lipscomb JD, Valentine M, Munck E, Hooper AB (1986) Tetraheme cytochrome c-554 from *Nitrosomonas europaea* - heme-heme interactions and ligand-binding. J Biol Chem 261: 1126–1138.
34. Edman P (1950) Method for determination of the amino acid sequence in peptides. Acta Chem Scand 4: 283–293.
35. Bendtsen JD, Nielsen H, von Heijne G, Brunak S (2004) Improved prediction of signal peptides: SignalP 3.0. J Mol Biol 340: 783–795.
36. Gasteiger EHC, Gattiker A, Duvaud S, Wilkins MR, Appel RD, et al. (2005) Protein Identification and Analysis Tools on the ExPASy Server. In: Walker JM, ed. The Proteomics Protocols Handbook. TotowaNew Jersey: Humana Press. pp 571–607.
37. Sogabe S, Miki K (1995) Refined crystal-structure of ferrocytochrome-*c*(2) from *Rhodopseudomonas viridis* at 1.6 angstrom resolution. J Mol Biol 252: 235–247.
38. Banci L, Bertini I, Rosato A, Varani G (1999) Mitochondrial cytochromes *c*: a comparative analysis. J Biol Inorg Chem 4: 824–837.
39. Walker FA (1999) Magnetic spectroscopic (EPR, ESEEM, Mossbauer, MCD and NMR) studies of low-spin ferriheme centers and their corresponding heme proteins. Coord Chem Rev 186: 471–534.
40. de Vries S, Albracht SPJ (1979) Intensity of Highly Anisotropic Low-Spin Heme EPR Signals. Biochim Biophys Acta 546: 334–340.
41. Taylor CPS (1977) EPR of Low-Spin heme Complexes - Relation of t2g Hole Model to Directional Properties of g-tensor, and a New Method for Calculating Ligand Field parameters. Biochim Biophys Acta 491: 137–149.

42. Zoppellaro G, Bren KL, Ensign AA, Harbitz E, Kaur R, et al. (2009) Studies of Ferric Heme Proteins with Highly Anisotropic/Highly Axial Low Spin (S = 1/2) Electron Paramagnetic Resonance Signals with bis-Histidine and Histidine-Methionine Axial Iron Coordination. Biopolymers 91: 1064–1082.
43. Brudvig GW (1995) Electron paramagnetic resonance spectroscopy. Meth Enzymol 246: 536–554.
44. Zoppellaro G, Teschner T, Harbitz E, Schuenemann V, Karlsen S, et al. (2006) Low-temperature EPR and Mossbauer spectroscopy of two cytochromes with His-Met axial coordination exhibiting HALS signals. ChemPhysChem 7: 1258–1267.
45. Zoppellaro G, Harbitz E, Kaur R, Ensign AA, Bren KL, et al. (2008) Modulation of the Ligand-Field Anisotropy in a Series of Ferric Low-Spin Cytochrome c Mutants derived from *Pseudomonas aeruginosa* Cytochrome c-551 and *Nitrosomonas europaea* Cytochrome *c*-552: A Nuclear Magnetic Resonance and Electron Paramagnetic Resonance Study. J Am Chem Soc 130: 15348–15360.
46. Bothe H, Jensen KM, Mergel A, Larsen J, Jorgensen C, et al. (2002) Heterotrophic bacteria growing in association with *Methylococcus capsulatus* (Bath) in a single cell protein production process. Appl Microbiol Biotechnol 59: 33–39.
47. Ambler RP, Dalton H, Meyer TE, Bartsch RG, Kamen MD (1986) The Amino Acid Sequence of Cytochrome cis-555 from the Methane Oxidizing Bacterium *Methylococcus Capsulatus* Biochem J 233: 333–337.
48. Yatsunyk LA, Carducci MD, Walker FA (2003) Low-spin ferriheme models of the cytochromes: Correlation of molecular structure with EPR spectral type. J Am Chem Soc 125: 15986–16005.
49. Berry EA, Walker FA (2008) Bis-histidine-coordinated hemes in four-helix bundles: how the geometry of the bundle controls the axial imidazole plane orientations in transmembrane cytochromes of mitochondrial complexes II and III and related proteins. J Biol Inorg Chem 13: 481–498.
50. Hooper AB, Dispirito AA (1985) In Bacteria Which Grows on Simple Reductants, Generation of a Proton Gradient Involves Extracytoplasmic Oxidation of Substrate. Microbiol Rev 49: 140–157.
51. Tonge GM, Harrison DEF, Higgins IJ (1977) Purification and Properties of Methane Mono-oxygenase Enzyme System from *Methylosinus trichosporium* OB3b Biochem J 161: 333–344.
52. Andersson SGE, Zomorodipour A, Andersson JO, Sicheritz-Ponten T, Alsmark UCM, et al. (1998) The genome sequence of *Rickettsia prowazekii* and the origin of mitochondria. Nature 396: 133–140.
53. Salmeen I, Palmer G (1968) Electron Paramagnetic resonance of Beef Heart Ferricytochrome *c*. J Chem Phys 48: 2049–2052.
54. Drepper F, Mathis P (1997) Structure and function of cytochrome c(2) in electron transfer complexes with the photosynthetic reaction center of *Rhodobacter sphaeroides*: Optical linear dichroism and EPR. Biochemistry 36: 1428–1440.
55. Axelrod HL, Feher G, Allen JP, Chirino AJ, Day MW, et al. (1994) Crystallization and X-ray structure of cytochrome c2 from *Rhodobacter sphaeroides* in 3 Crystal Forms. Acta Crystallogr D 50: 596–602.
56. Hederstedt L, Andersson KK (1986) Electron Parapmagnetic Resonance Spectroscopy of *Bacillus subtilis* Cytochrome b558 in *Escherichia coli* Membranes and in Succinate Dehydrogenase Complex from *Bacillus subtilis* Membranes. J Bacteriol 167: 735–739.

II

III

IV